Cell Genomics

Article

Polygenic prediction across populations is influenced by ancestry, genetic architecture, and methodology

Graphical abstract

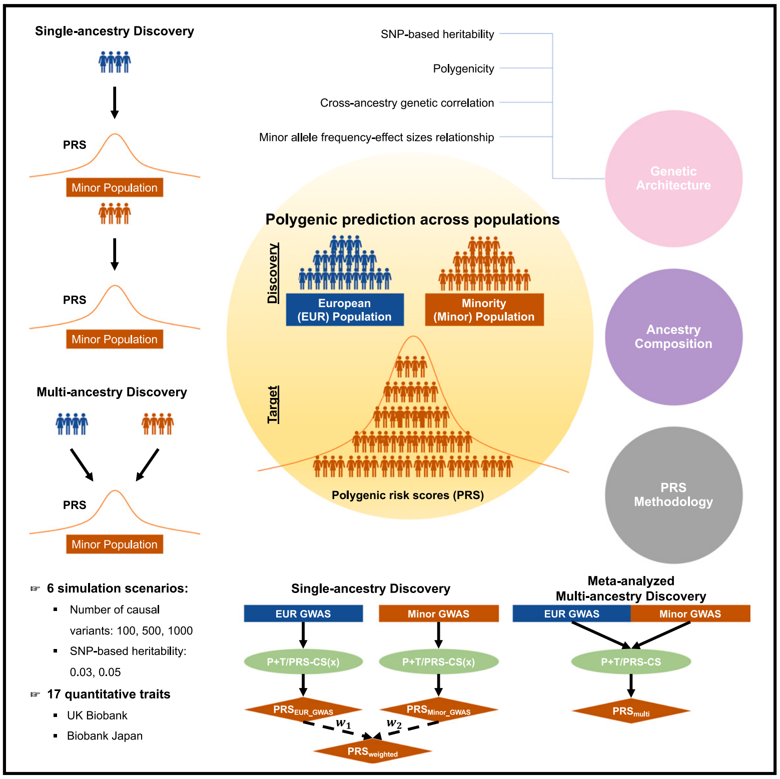

Highlights

- PRSs derived from multi-ancestry GWASs improved accuracy in understudied populations
- Multi-ancestry GWAS-based PRSs outperformed weighted PRSs from single-ancestry GWASs
- Local ancestry-informed PRSs enhanced predictive performance in African populations
- Best practices for utilizing genomic diversity for PRS prediction were provided

Authors

Ying Wang, Masahiro Kanai,
Taotao Tan, ..., Patrick Turley,
Elizabeth G. Atkinson, Alicia R. Martin

Correspondence

yiwang@broadinstitute.org (Y.W.),
armartin@broadinstitute.org (A.R.M.)

In brief

Wang et al. conducted extensive simulations and empirical analyses, revealing that incorporating greater diversity from discovery GWASs improved PRS accuracy in comparison to using large-scale, European-based PRSs in understudied populations. They also offered valuable guidelines for optimizing polygenic prediction across diverse populations, considering genetic architecture, ancestry composition, and PRS methodologies.

Wang et al., 2023, Cell Genomics *3*, 100408
October 11, 2023 © 2023 The Authors.
https://doi.org/10.1016/j.xgen.2023.100408

Cell Genomics

CellPress
OPEN ACCESS

Article

Polygenic prediction across populations is influenced by ancestry, genetic architecture, and methodology

Ying Wang,[1,2,11,*] Masahiro Kanai,[1,2,3,4] Taotao Tan,[5] Mireille Kamariza,[6] Kristin Tsuo,[1,2] Kai Yuan,[1,2] Wei Zhou,[1,2] Yukinori Okada,[4,7,8,9] the BioBank Japan Project, Hailiang Huang,[1,2] Patrick Turley,[10] Elizabeth G. Atkinson,[5] and Alicia R. Martin[1,2,*]

[1]Analytic and Translational Genetics Unit, Massachusetts General Hospital, Boston, MA 02114, USA
[2]Stanley Center for Psychiatric Research and Program in Medical and Population Genetics, Broad Institute of MIT and Harvard, Cambridge, MA 02142, USA
[3]Department of Biomedical Informatics, Harvard Medical School, Boston, MA, USA
[4]Department of Statistical Genetics, Osaka University Graduate School of Medicine, Suita, Japan
[5]Department of Molecular and Human Genetics, Baylor College of Medicine, Houston, TX, USA
[6]Society of Fellows, Harvard University, Cambridge, MA 02138, USA
[7]Laboratory for Systems Genetics, RIKEN Center for Integrative Medical Sciences, Yokohama, Japan
[8]Laboratory of Statistical Immunology, Immunology Frontier Research Center (WPI-IFReC), Center for Infectious Disease Education and Research (CiDER), and Integrated Frontier Research for Medical Science Division, Institute for Open and Transdisciplinary Research Initiatives, Osaka University, Suita 565-0871, Japan
[9]Department of Genome Informatics, Graduate School of Medicine, the University of Tokyo, Tokyo 113-0033, Japan
[10]Department of Economics, and Center for Economic and Social Research, University of Southern California, Los Angeles, CA, USA
[11]Lead contact
*Correspondence: yiwang@broadinstitute.org (Y.W.), armartin@broadinstitute.org (A.R.M.)

https://doi.org/10.1016/j.xgen.2023.100408

SUMMARY

Polygenic risk scores (PRSs) developed from multi-ancestry genome-wide association studies (GWASs), PRS$_{multi}$, hold promise for improving PRS accuracy and generalizability across populations. To establish best practices for leveraging the increasing diversity of genomic studies, we investigated how various factors affect the performance of PRS$_{multi}$ compared with PRSs constructed from single-ancestry GWASs (PRS$_{single}$). Through extensive simulations and empirical analyses, we showed that PRS$_{multi}$ overall outperformed PRS$_{single}$ in understudied populations, except when the understudied population represented a small proportion of the multi-ancestry GWAS. Furthermore, integrating PRSs based on local ancestry-informed GWASs and large-scale, European-based PRSs improved predictive performance in understudied African populations, especially for less polygenic traits with large-effect ancestry-enriched variants. Our work highlights the importance of diversifying genomic studies to achieve equitable PRS performance across ancestral populations and provides guidance for developing PRSs from multiple studies.

INTRODUCTION

Polygenic risk scores (PRSs) are useful tools for estimating the cumulative genetic susceptibility to complex traits and diseases. PRSs are typically calculated by weighting the number of risk alleles based on their associations in genome-wide association studies (GWASs). PRSs have shown promising potential in predicting some traits and disease risks, comparable to monogenic variants and traditional clinical risk factors.[1–5] Achieving the most accurate and generalizable PRS requires access to large-scale and diverse GWASs, especially with representation that matches the specific target population. However, the current landscape of GWASs predominantly focuses on European (EUR) ancestry populations, which have considerably larger sample sizes compared with other populations. Although ongoing efforts are underway to rectify these gaps, achieving global representativeness is a challenging goal. Encouragingly, studies have shown that using GWAS data with even a small proportion of non-EUR-ancestry individuals has the potential to improve the predictive accuracy of PRSs in underrepresented populations.[6–8] This finding could largely be attributed to the substantial contribution of common variants to the heritable variation of complex traits and diseases and that causal variants are largely shared across ancestries.[9–12] With the ever-increasing availability and scalability of genomic data from underrepresented and ancestrally diverse populations, we are especially interested in leveraging this greater diversity to improve PRS generalizability.

In particular, recently admixed populations, consisting of chromosomal segments of mosaic ancestries, are systematically excluded in many existing genomic studies due to their underrepresentation and complicated population structure.[13–15] However, these populations present unique opportunities to develop more generalizable PRSs, as their genetic effects can be estimated in more consistent environments, which helps reduce confounding factors compared with estimates across different ancestry groups in different populations.[16] Furthermore, the comprehensive characterization of phenotypes is often insufficient or inconsistently performed in different populations. However, in the recently admixed populations, there is a greater potential for consistency and comparability in phenotype measurements, as the genetic factors contributing to phenotypic differences between the source populations can be decoupled in the recently admixed populations.[16,17] The advancement of methodologies such as local ancestry inference and association testing has further enabled ancestry-specific GWASs in admixed populations,[18–20] allowing for the construction of PRSs that leverage genetic information captured by local ancestry inference. With the ongoing data accumulation from recently admixed populations, particularly through initiatives like the All of Us Research Program,[21] expanded resources will provide unparalleled opportunities to explore the performance of PRSs derived from local ancestry-informed summary statistics within historically underrepresented populations. Furthermore, such data will facilitate their integration with PRSs derived from predominantly EUR-based cohorts.

Recently developed statistical methodologies leverage the increasing diversity of GWAS data to improve PRS portability.[8,22,23] However, the effect of genetic architecture, ancestry composition of GWAS discovery cohorts, and PRS construction methodologies on cross-ancestry predictive accuracy remains largely unclear. For example, a recent study found no increase in accuracy when meta-analyzing GWASs from a relatively small Ugandan cohort with larger EUR data.[6] Furthermore, theoretical frameworks for approximating expected PRS accuracy from multi-ancestry GWASs are lacking. Current theoretical calculations for PRS accuracy rely on the assumption of homogeneity within the ancestral discovery samples,[24,25] ignoring factors that are likely to play a role in multi-ancestry cohorts. Such factors may include differences in linkage disequilibrium (LD), minor allele frequency (MAF), heritability, sample sizes, and genetic correlation across different ancestries.

To provide insights into those issues, we explored the impact of ancestry compositions in discovery GWASs on the predictive accuracy of PRSs constructed using different methodologies. This exploration involved large-scale population genetic simulations as well as the utilization of real genomic data from the BioBank Japan (BBJ)[26] and UK Biobank (UKBB)[27] across traits exhibiting distinct genetic architectures (Figure 1). In what follows, we used single-ancestry GWASs to denote studies conducted exclusively within a single ancestry group (defined using genetic data), while multi-ancestry GWASs refer to studies encompassing two or more distinct ancestries. In our analyses, we performed meta-analyses of GWASs conducted in EUR ancestry populations (EUR GWASs) and GWASs conducted in other minority populations (Minor GWASs) by varying the ratios of sample sizes to mimic multi-ancestry GWASs with varying ancestry compositions. Specifically, we focused on East Asian (EAS) and African (AFR) minority populations. By comparing the performance of PRSs derived from single-ancestry GWASs (referred to as $\mathrm{PRS}_{\mathrm{single}}$) and multi-ancestry GWASs (referred to as $\mathrm{PRS}_{\mathrm{multi}}$) through simulations and real data, we consistently observed that $\mathrm{PRS}_{\mathrm{multi}}$ overall exhibited superior performance in comparison to $\mathrm{PRS}_{\mathrm{single}}$ (primarily PRSs derived from large-scale EUR GWASs, referred to as $\mathrm{PRS}_{\mathrm{EUR\_GWAS}}$). As admixed populations remain understudied despite disproportionately yielding novel genetic findings,[28] we further conducted local ancestry inference to explore whether, how, and to what extent PRS performance could be improved using GWAS discovery data from AFR-EUR admixed individuals. While optimal PRS methods are trait and context specific, this study comprehensively evaluates PRS accuracy across a wide range of scenarios, facilitating a set of best practices that ultimately reduce the number of analyses necessary to optimize PRSs for specific applications.

RESULTS

Evaluating the effects of imbalanced sample sizes across ancestries on PRS accuracy through simulations

We simulated genotypes using HapGen2 and phenotypes by varying trait heritability (h^2 = 0.03, 0.05) and number of causal variants (M_c = 100, 500, 1,000), such that the polygenicity ranged from ∼0.1% to ∼1%. We assumed that the causal variants and their effect sizes are shared across ancestries (i.e., cross-ancestry genetic correlation [r_g] is 1) in our initial simulations. For single-ancestry GWASs, we first conducted GWASs within each bin and then meta-analyzed GWASs across different numbers of bins (1–52 per ancestry). Each bin represented 10,000 individuals randomly sampled from the corresponding ancestry. For multi-ancestry GWASs, we meta-analyzed GWASs from EUR and minor populations (EAS or AFR) to evaluate the impact of ancestry composition. We used varying numbers of bins from the EUR GWASs (4–52 with 4 increments) and varied the contribution from EAS or AFR GWASs (1–52 bins). We constructed PRSs using the classic pruning and thresholding (P + T) method with varying p value thresholds. We assessed the accuracy, measured by prediction R^2, using the optimal threshold through fine-tuning in the validation cohort. The detailed simulation setup is shown in Figure 1 and STAR Methods.

PRS predictive accuracy improved with more individuals from target populations included in the multi-ancestry GWASs but varied with genetic architecture

When developing $\mathrm{PRS}_{\mathrm{single}}$, we found that using ancestry-matched GWASs generally outperformed using GWASs from other discovery populations (Figure S1). Compared to using EUR GWASs, the benefit of using ancestry-matched GWASs was more evident for traits with more polygenic genetic architectures and larger GWAS sample sizes. To further evaluate the impact of ancestry composition, we compared the accuracy of $\mathrm{PRS}_{\mathrm{multi}}$ and $\mathrm{PRS}_{\mathrm{single}}$. We constructed $\mathrm{PRS}_{\mathrm{multi}}$ using an LD reference panel consisting of individuals proportional to the ancestry composition of the discovery GWAS (STAR Methods). This reference panel yielded approximately optimal accuracy among three different reference panels utilized in our study (Figure S2).

Relative to the accuracy of $\mathrm{PRS}_{\mathrm{EUR\_GWAS}}$, we observed significant improvements in the understudied population by including

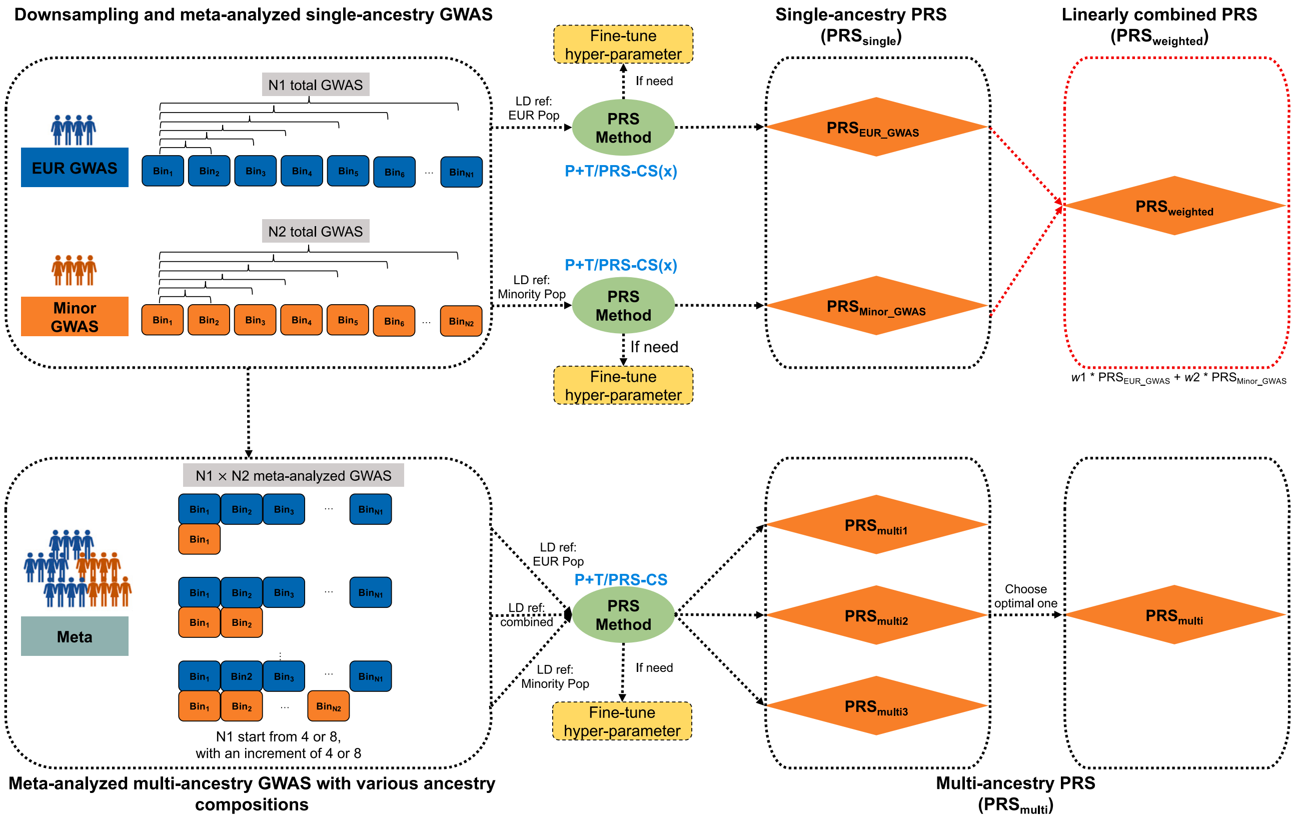
Downsampling and meta-analyzed single-ancestry GWAS
N1 total GWAS
EUR GWAS
Bin1 Bin2 Bin3 Bin4 Bin5 Bin6 ... BinN1
N2 total GWAS
Minor GWAS
Bin1 Bin2 Bin3 Bin4 Bin5 Bin6 ... BinN2
Fine-tune hyper-parameter
If need
LD ref: EUR Pop
PRS Method
P+T/PRS-CS(x)
LD ref: Minority Pop
Single-ancestry PRS (PRSsingle)
PRSEUR_GWAS
PRSMinor_GWAS
Linearly combined PRS (PRSweighted)
PRSweighted
w1 * PRSEUR_GWAS + w2 * PRSMinor_GWAS
N1 × N2 meta-analyzed GWAS
Meta
N1 start from 4 or 8, with an increment of 4 or 8
Meta-analyzed multi-ancestry GWAS with various ancestry compositions
LD ref: combined
P+T/PRS-CS
PRSmulti1
PRSmulti2
PRSmulti3
Choose optimal one
PRSmulti
Multi-ancestry PRS (PRSmulti)

Figure 1. Study design in both simulations and empirical analyses

(1) In the context of single-ancestry GWASs, we randomly split individuals in European (EUR) and other minority populations, including East Asian and African populations, into equally sized bins. Simulations involved a total of 52 bins per population, each containing 10,000 individuals. For empirical analysis, bin number was dependent on the sample size of the respective phenotype in that population (Table S3), with 5,000 individuals per bin. A GWAS was conducted within each bin for each individual population, followed by meta-analysis of GWASs from various numbers of bins within each population. To construct PRSs derived from single-ancestry GWASs (PRS_{single}) in the target population, we applied P + T for both simulations and empirical analyses, utilizing PRS-CS for the latter. Subsequently, we combined PRS_{single} developed from EUR GWAS (PRS_{EUR_GWAS}) and other minority population-based GWAS (PRS_{Minor_GWAS}) through a linear weighted strategy (denoted as $PRS_{weighted}$, highlighted in red box) for empirical analyses. Note that $PRS_{weighted}$ was also developed using PRS-CSx, which utilizes GWAS summary statistics from multiple populations. (2) For meta-analyzed multi-ancestry GWASs (referred to as Meta), we ran meta-analyses on EUR GWASs and Minor GWASs with varying ancestry compositions. In simulations, we incrementally included 4 bins from EUR GWASs for the meta-analysis, while in empirical analyses, we increased the number to 8 bins. Simultaneously, we varied the number of bins in Minor GWASs from 1 to the total number. Following the meta-analysis, we constructed PRSs based on Meta (referred to as PRS_{multi}), using the P + T method for simulations, and employing both P + T and PRS-CS for empirical analyses.

more individuals from the target ancestry in multi-ancestry GWASs. Across all simulations, a statistically significant median improvement of 0.008 in R^2 was observed (one-sided Wilcoxon signed-rank test, $p < 2.2e-16$; Table S1). This trend was more apparent in more polygenic traits. As shown in Figure 2, we compared accuracy between PRS_{multi} and PRS_{EUR_GWAS} derived from 320,000 EUR individuals. For traits with an h^2 of 0.05, the median improvements in R^2 of PRS_{multi} were 0.006, 0.014, and 0.013 with M_c of 100, 500, and 1,000, respectively, in EAS individuals. Similarly, corresponding R^2 improvements of 0.009, 0.010, and 0.014 were shown in AFR individuals (Figure S3). However, we did not consistently observe such accuracy gains for the majority EUR population or in scenarios where the other understudied ancestry was not included in the multi-ancestry discovery GWAS. In our simulations, but unlike in most GWASs, populations typically understudied in current genomic studies can be the majority in the discovery GWASs. Note that when the proportion of underrepresented populations in the discovery GWAS was below 50%, we still observed significant improvements in PRS accuracy. Specifically, across various simulations, we noted a median increase in R^2 of 0.007 ($p < 2.2e-16$). We expected to observe similar relative R^2 improvements, which measured the PRS generalizability, in the target populations using PRS_{multi} compared with using PRS_{EUR_GWAS} (STAR Methods).

Compared with using PRS_{EUR_GWAS}, we found that PRS_{multi} derived from GWASs with much smaller sample sizes could achieve comparable or better predictive accuracy (Table S1). For example, in the scenario with an M_c of 1,000 and an h^2 of 0.03, the meta-analysis of 16 EUR and 2 AFR bins achieved a comparable accuracy of 0.008 to that of using 32 EUR bins in the AFR population. Overall, adding fewer individuals from the

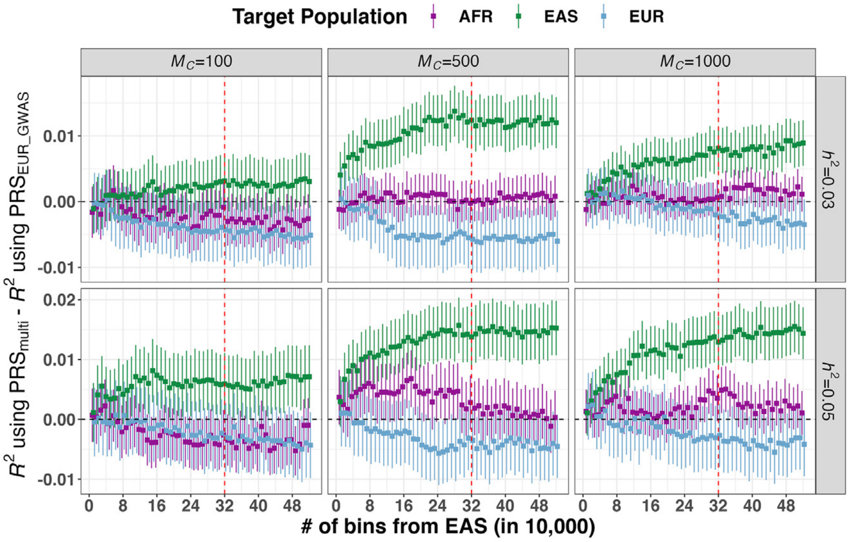

Figure 2. Improvement of PRS accuracy through meta-analyzed multi-ancestry GWASs compared with large-scale EUR GWASs across 6 simulated genetic architectures

The multi-ancestry GWASs included populations of EUR and East Asian (EAS) ancestry, with the EAS sample size varying as indicated on the x axis. For illustrative purposes, we present the results using 32 EUR bins, each consisting of 10,000 individuals, which were included in both EUR GWASs and multi-ancestry GWASs. The PRS was separately evaluated in African (AFR), EAS, and EUR populations. Full results are shown in Table S1. M_c indicates the number of causal variants, and h^2 refers to SNP-based heritability. In each panel, the red vertical dashed line indicates the point where an equal number of bins from EUR and EAS populations was included in the multi-ancestry GWAS. The error bars represent the SEs of predictive accuracy differences between PRS_{multi} and PRS_{EUR_GWAS}.

target populations saturated accuracy improvements faster for less polygenic traits than more polygenic traits. Similarly, larger sample sizes from AFR populations were required to achieve comparable accuracy to EAS populations, especially for more polygenic traits, likely due to the larger effective population size in AFR populations and larger genetic divergence between EUR and AFR populations. As shown in Figure S3, when h^2 was 0.03, the accuracy improvement of PRS_{multi} in AFR plateaued to ~0.005 with 11 and 20 AFR bins for M_c of 100 and 500, respectively, but continued to increase with more AFR bins for an M_c of 1,000. Similarly, when h^2 was 0.03, including 2 and 12 EAS bins in PRS_{multi} yielded an accuracy improvement of >0.005 in EAS for M_c of 100 and 500, respectively (Figure 2). In comparison to PRSs derived from Minor GWASs alone (PRS_{Minor_GWAS}), we found that the accuracy improvement of PRS_{multi} gradually diminished as the sample size of Minor GWASs increased (Figure S4; Table S1). We showed that for more polygenic traits, PRS_{multi} achieved little to no improvement when the understudied target populations accounted for more than half of the sample size in multi-ancestry GWASs.

Because r_g estimates can be significantly less than 1, we also modified our simulations by varying the r_g to be 0.6 and 0.8. We investigated two simulation scenarios that represent the extremes in per-variant variance explained: the least polygenic scenario 1 with M_C = 100 and h^2 = 0.05, and the most polygenic scenario 2 with M_C = 1,000 and h^2 = 0.03 (STAR Methods). Consistent with our previous findings, PRS_{multi} exhibited improved accuracy in the target population when a greater number of individuals from the same ancestry were included, as compared to relying solely on large-scale EUR GWASs (Figures S5A and S5B; Table S2). This improvement was more pronounced for scenario 2. Moreover, we needed a larger number of individuals from the target ancestry to saturate accuracy improvements in scenario 1 when r_g was moderately reduced. Furthermore, as the sample sizes of the Minor GWASs increased and the values of r_g decreased, the advantage of utilizing PRS_{multi} over PRS_{Minor_GWAS} diminished and eventually vanished (Figures S5C and S5D; Table S2).

Empirical analysis of PRS accuracy within and across ancestries using 17 quantitative phenotypes

Genetic architecture of 17 studied phenotypes

To understand how trait genetic architecture influences the accuracy of PRSs across ancestries, we conducted a comprehensive analysis involving 17 phenotypes in the UKBB and the BBJ. Using the summary-data-based BayesS (SBayesS) method, we estimated key parameters, including SNP-based heritability, polygenicity (the proportion of SNPs with nonzero effects), and a coefficient of negative selection (*S*; measuring the relationship between MAF and estimated effect sizes), by leveraging GWAS summary statistics as input data.[29]

The phenotypes included in this study varied widely in genetic architecture across these estimated parameters (Figure 3; Tables S3 and S4). The polygenicity estimates spanned a broad range, from low values (0.001–0.005) for traits like mean corpuscular hemoglobin concentration (MCHC), basophil count (basophil), mean corpuscular hemoglobin (MCH), and mean corpuscular volume (MCV), to higher values (0.012–0.047) for traits such as height and body mass index (BMI). SNP-based heritability estimates similarly ranged from <0.1 for basophil and MCHC to 0.54 and 0.33 for height using the UKBB and the BBJ, respectively, regardless of polygenicity. The median *S* parameters were −0.63 and −0.47 using the UKBB and the BBJ, respectively. While the negative *S* values indicate negative selection (i.e., rarer variants have larger effects), it remains unclear to what degree population stratification could confound such estimates.[30,31] We found that the polygenicity estimates using the UKBB were mostly higher than those using the BBJ, which could be due to the higher statistical power with larger sample sizes in the UKBB resulting in the detection of more variants with small effects. Similarly, we observed significantly higher SNP-based heritability in the UKBB compared with the BBJ, with the exception of MCHC and basophil, indicating

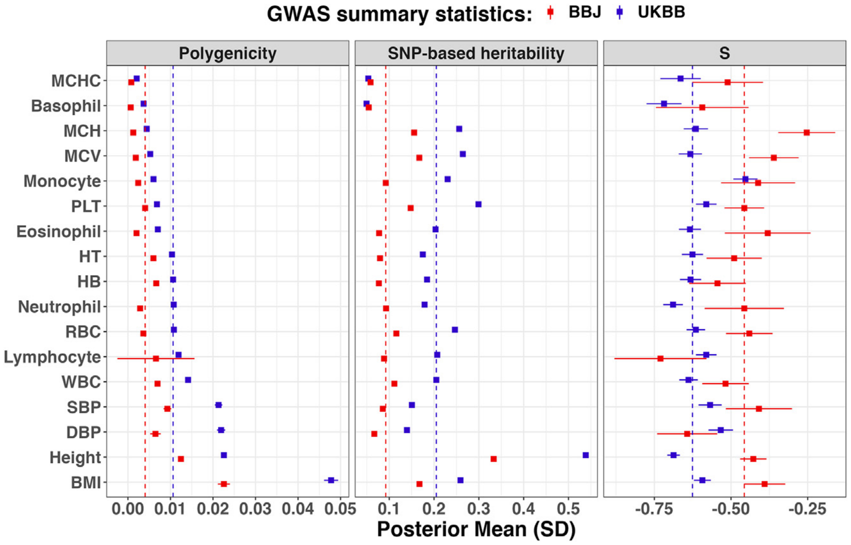

Figure 3. Genetic architecture of 17 studied traits between the BioBank Japan and the UK Biobank

The error bar is the standard deviation of the corresponding estimate. The vertical dashed line was the median estimate. Full results are shown in Table S4. The phenotypes were ranked according to their polygenicity estimates using GWASs from the UKBB, including: BMI (body mass index); height; DBP (diastolic blood pressure); SBP (systolic blood pressure); WBC (white blood cell count); lymphocyte (lymphocyte count); RBC (red blood cell count); neutrophil (neutrophil count); HB (hemoglobin concentration); HT (hematocrit percentage); eosinophil (eosinophil count); PLT (platelet count); monocyte (monocyte count); MCV (mean corpuscular volume); MCH (mean corpuscular hemoglobin); basophil (basophil count); and MCHC (mean corpuscular hemoglobin concentration).

possible phenotype heterogeneity between the two cohorts. These results are expected from the biobank designs, as the BBJ is a hospital-based cohort with participants recruited with certain diseases, whereas the UKBB is a population-based cohort with overall healthier participants and thus a wider range of natural variation in complete blood counts. This finding is also consistent with the previous study using estimates from LD score regression (LDSC) and stratified LDSC.[32] Moreover, the estimated r_g between the UKBB and the BBJ for those traits were not statistically different from 1 ($p > 0.05/17$) except for a few including basophil (0.5945, SE = 0.1221), height (0.6932, SE = 0.0172), BMI (0.7474, SE = 0.0230), diastolic blood pressure (DBP; 0.8354, SE = 0.0509), and systolic blood pressure (SBP; 0.8469, SE = 0.0430).[32]

PRS_{multi} usually improves predictive performance compared with PRS_{single}. We constructed PRS_{single} using P + T and PRS-continuous shrinkage (PRS-CS) with GWASs from the UKBB and the BBJ, respectively. The GWAS sample sizes varied based on the number of Bin_{Total}, which represented the total number of bins specific to each trait as shown in Table S3. Each bin consisted of 5,000 individuals randomly selected from the respective cohort. We found that employing target ancestry-matched GWASs, even with smaller sample sizes, yielded comparable accuracy to utilizing large-scale EUR GWASs but depended on PRS methodology and trait-specific genetic architecture (Figures S6 and S7; Table S5).

For comparison, we developed PRS_{multi} through meta-analyzing single-ancestry GWASs obtained from the UKBB and the BBJ. The PRS_{multi} was constructed by varying the number of bins from each cohort, with UKBB bins ranging from 8 to 64, incrementing by 8 (details provided in STAR Methods and Figure 1). Consistent with our findings from the simulations, where we observed that the choice of LD reference panel had limited impacts on the predictive accuracy of more polygenic traits, we observed only a slight improvement of median R^2 of 0.002 for P + T when employing a combined LD reference panel that was proportional to the ancestries represented in the multi-ancestry GWASs. We compared this result with PRSs developed using a reference panel that was matched with the majority population of the discovery GWAS (Figure S8; Table S6). Because the majority of PRSs (85%) were constructed from GWASs predominantly composed of EUR individuals (>50% EUR), we hereafter reported the results using 1KG-EUR as the LD reference.

In our analysis comprising 3,160 comparisons between PRSs derived from UKBB GWASs (PRS_{EUR_GWAS}) and PRS_{multi}, we observed encouraging results. Specifically, in the UKBB-EAS population, PRS_{multi} showed accuracy improvements in 99.7% and 92.4% of these comparisons when using P + T and PRS-CS, respectively (Table S7; Figure S9). Accuracy increased with more EAS samples in the multi-ancestry GWAS (Figure 4). For example, when comparing PRS_{multi} with PRS_{EUR_GWAS} using P + T, the largest relative improvements in R^2 were 80.9% (0.085 vs. 0.047) for platelet count (PLT), 152.2% (0.058 vs. 0.023) for BMI, and 91.9% (0.071 vs. 0.037) for height. We observed these improvements when using multi-ancestry GWASs including EAS bins from the BBJ, which were either concordant with or proximal to Bin_{Total}, along with 64 EUR bins from the UKBB. Similarly, the corresponding relative R^2 improvements for these same three traits were 18.9% (0.126 vs. 0.106), 50% (0.075 vs. 0.050), and 15.5% (0.097 vs. 0.084) when using PRS-CS. We did not consistently observe the upward trend for white blood cell count (WBC) with PRS-CS, which can be attributed to the lack of accuracy improvement with larger sample sizes of BBJ (Figure S6). We also found that P + T showed greater improvement compared to PRS-CS but worse accuracy overall, regardless of the number of bins from EUR GWASs; the median improvements in R^2 across traits were 0.014 and 0.008, respectively. However, the upward trend in PRS accuracy was not consistently shown in the UKBB-EUR, particularly when using PRS-CS (Figure S10; Table S7). This pattern aligned with our simulation results and previous reports that PRS accuracy for minority populations included in the multi-ancestry GWAS benefited more from adding more ancestry-matched individuals compared with other populations, including EUR populations.[33]

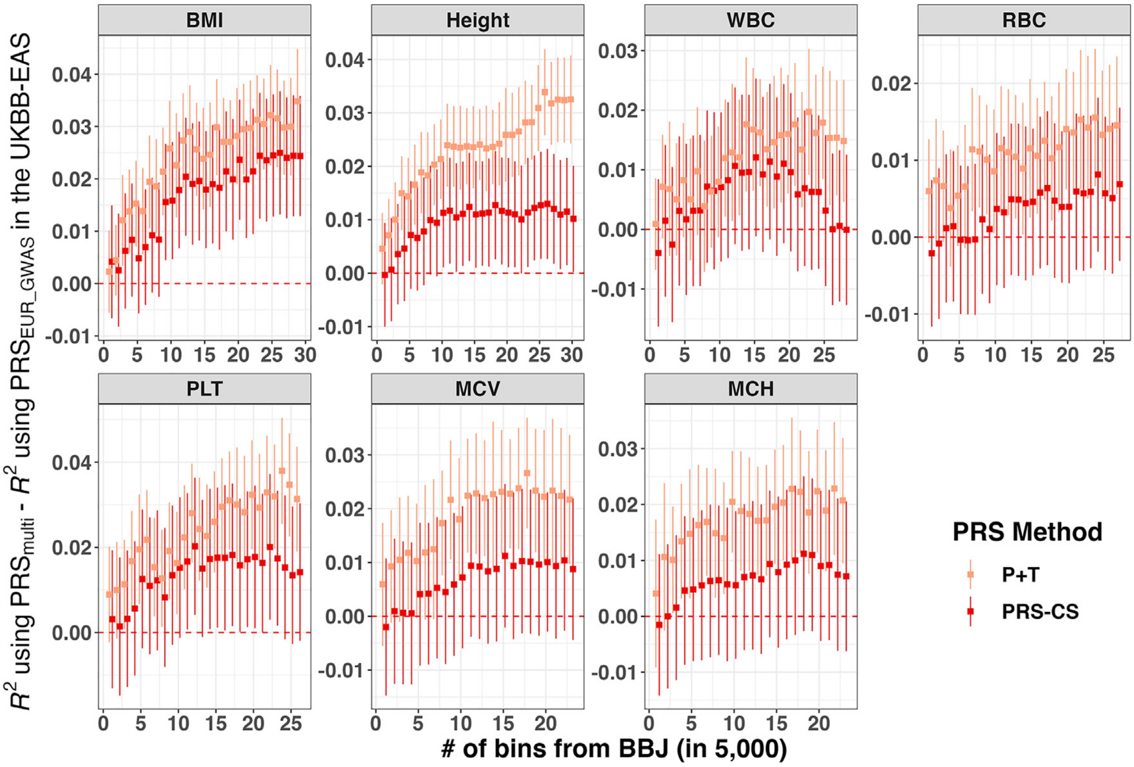

Figure 4. Accuracy improvement of PRS in the UKBB-EAS population using multi-ancestry GWASs compared with using EUR GWASs for P + T and PRS-CS

The multi-ancestry GWASs were obtained by meta-analyzing EUR GWASs and EAS GWASs, with the EAS sample size from the BBJ varying as indicated on the x axis. For illustrative purposes, we present the results using 64 EUR bins, each containing 5,000 individuals, which were included in both EUR GWASs and multi-ancestry GWASs. The y axis is the accuracy difference of PRSs when using multi-ancestry GWASs (PRS_{multi}) compared with using EUR GWASs (PRS_{EUR_GWAS}). The error bars indicate the SE of accuracy improvement. The red dashed line is y = 0. We showed the results for 7 traits with SNP-based heritability >0.1 in both the BBJ and the UKBB, and they were ranked by polygenicity estimates using the UKBB (Figure 3). Abbreviations are the same as in Figure 3. Full results are shown in Table S7.

We noted that the accuracy of PRS_{multi} remained largely unchanged or slightly decreased when the number of bins from the BBJ was small (e.g., 1 or 2 bins), which was consistent with previous studies.[6,33] In contrast to PRSs derived from the BBJ (PRS_{Minor_GWAS}), we noted a diminishing trend in accuracy improvements of PRS_{multi} as the sample sizes of BBJ increased, especially for traits such as height, PLT, MCH, and MCV (Figure S11). Furthermore, we observed greater variation in accuracy among traits from real data compared with simulations, which could be attributed to the smaller sample sizes and the more complicated genetic architecture.

PRSs derived from meta-analyzed multi-ancestry GWASs vs. weighted PRSs from single-ancestry GWASs in understudied populations. In contrast to PRS_{multi}, an alternative approach proposed in previous studies to enhance predictive accuracy in diverse populations is the linear combination of PRSs derived from GWASs conducted on populations with different ancestries.[34] Here, we implemented this approach by developing a weighted PRS ($PRS_{weighted}$) using P + T and PRS-CS. This combination involved linearly weighting PRSs derived from single-ancestry GWASs conducted in the UKBB and the BBJ. Additionally, we employed a more advanced Bayesian method called PRS-CSx,[8] which jointly models GWAS and LD information from multiple populations. Similarly, we constructed $PRS_{weighted}$ using ancestry-specific posterior SNP effects. Furthermore, we developed PRSs by integrating ancestry-specific posterior SNP effects using the inverse-variance weighted meta-analysis strategy, also referred to as PRS_{multi} (see STAR Methods).

Among the three PRS methods evaluated in the UKBB-EAS, PRS-CSx exhibited the highest performance, followed by PRS-CS and P + T. Specifically, for PRS_{multi}, the corresponding median R^2 values across traits were 0.051, 0.048, and 0.037, while for $PRS_{weighted}$, they were 0.051, 0.045, and 0.021, respectively (Figure 5; Tables S8 and S9). Notably, we observed that PRS_{multi} for BMI using PRS-CS yielded significantly better accuracy compared with PRS-CSx (median R^2: 0.057 vs. 0.055, $p < 2.2e-16$). Out of the 3,160 comparisons between PRS_{multi} and $PRS_{weighted}$ in the UKBB-EAS, 91.4% and 78% showed higher accuracy of PRS_{multi} ($p < 2.2e-16$) when using P + T and PRS-CS, respectively, with median improvements in R^2 of 0.011 and 0.003. Although we found better performance overall with PRS_{multi}, we found that $PRS_{weighted}$ significantly outperformed PRS_{multi} for PLT using P + T (median R^2: 0.086 vs. 0.081, $p < 2.2e-16$) and for height using PRS-CS (median

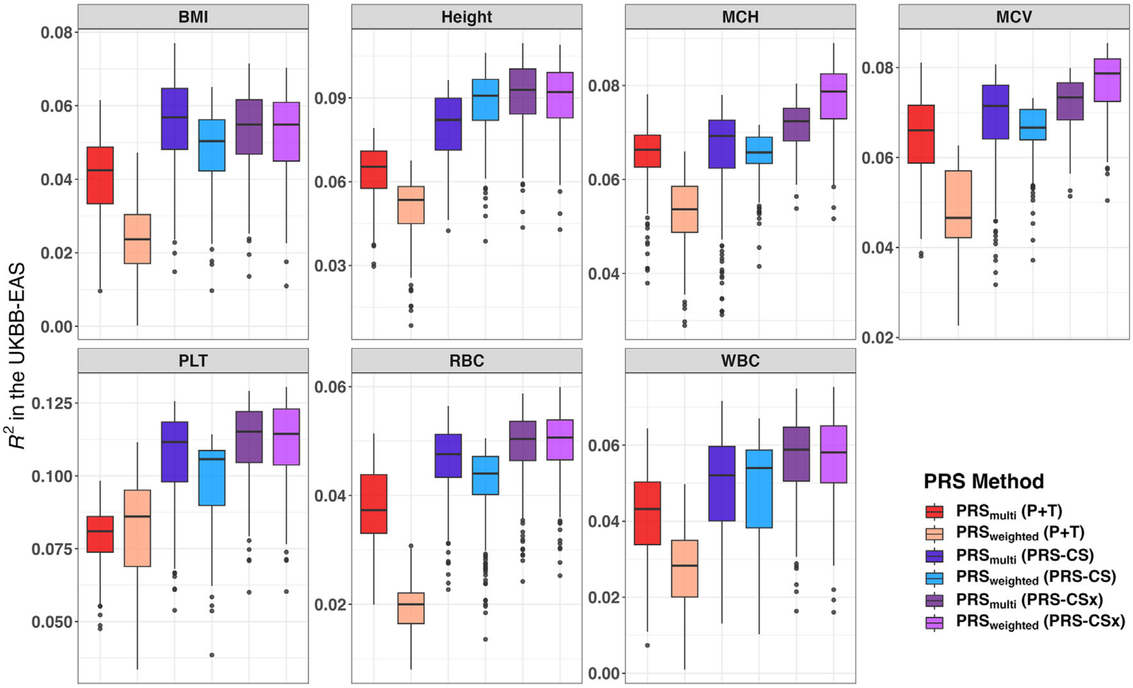

Figure 5. Predictive accuracy using different PRS methods in the UKBB-EAS population

We showed the results for 7 traits with SNP-based heritability >0.1 in both the BBJ and the UKBB. Traits were ranked by polygenicity estimates using the UKBB (Figure 3). Boxes represent the first and third quartiles, with the whiskers extending to 1.5-fold the interquartile range. Abbreviations are the same as in Figure 3. Full results are shown in Tables S8 and S9.

R^2: 0.091 vs. 0.082, p = 2.6e−04). Contrary to trends observed with other methods, in 59.7% of the comparisons, $PRS_{weighted}$ outperformed PRS_{multi} when using PRS-CSx, although we observed no significant accuracy difference across traits. However, $PRS_{weighted}$ showed superior performance compared with PRS_{multi} ($p < 0.05/17$) for several traits, including MCV (median R^2: 079 vs. 0.072), MCH (median R^2: 0.079 vs. 0.073), basophil (median R^2: 0.010 vs. 0.007), and hemoglobin (HB) concentration (median R^2: 0.025 vs. 0.024).

Moreover, the extent of accuracy improvements using PRS_{multi}, in contrast to $PRS_{weighted}$, largely varied across traits and ancestry compositions. For example, when evaluating accuracy within the UKBB-EAS using P + T, we observed 3.25-fold increase in R^2 with PRS_{multi} compared with $PRS_{weighted}$ for monocyte count (monocyte; 0.065 vs. 0.020). This improvement was achieved with a bin ratio 56:15 for the discovery GWAS, consisting of 56 bins from the UKBB and 15 bins from the BBJ. Similarly, using a bin ratio of 40:25, we achieved a 4-fold increase in R^2 for DBP (0.048 vs. 0.012) with PRS_{multi} compared with $PRS_{weighted}$. When developing PRS_{multi} using PRS-CS, we observed notable relative improvements in R^2 when compared to $PRS_{weighted}$, specifically a 24.7% increase for PLT (0.091 vs. 0.073) with a bin ratio of 24:1 and a 57.1% increase for lymphocyte (0.044 vs. 0.028) with a bin ratio of 16:1. Additionally, we found that PRS-CSx showed better performance in comparison with PRS-CS, especially when the EUR GWAS was smaller or the Minor GWAS was larger. However, such improvements were less pronounced with large-scale EUR GWASs or small Minor GWASs (Figure S12). While sharing ancestry-specific GWAS summary statistics is highly beneficial for determining optimal approaches, our findings highlight the value of pragmatic approaches that directly construct PRS from large-scale meta-analyzed multi-ancestry GWASs. Such studies are often more accessible than ancestry-specific GWAS summary statistics.

PRSs derived from local ancestry-informed GWASs can improve accuracy for some less polygenic traits

We next conducted a comparative analysis to evaluate the optimal PRS approaches for admixed populations, utilizing local ancestry-informed GWASs. Specifically, we used Tractor[19] to perform GWASs in AFR tracts within admixed AFR-EUR individuals, referred to as $AFR_{Tractor}$. This approach enabled us to construct ancestry-specific PRSs across 17 traits in the understudied AFR population. We developed PRSs using both P + T and PRS-CS and subsequently compared the accuracies of PRSs derived from $AFR_{Tractor}$ with those derived from large-scale EUR GWASs performed with standard linear regression ($EUR_{standard}$). To maximize discovery sample size, we also developed $PRS_{weighted}$ by combining $EUR_{standard}$-derived PRSs and $AFR_{Tractor}$-derived PRSs through linear weighting; we compared its performance with PRSs derived from multi-ancestry meta-analyzed GWAS (referred to as $Meta_{standard}$; see STAR Methods).

Local ancestry-informed ancestry-specific GWASs had a much smaller sample size relative to the EUR-inclusive GWASs, as is typical for GWASs of underrepresented populations. As expected, we did not observe significant predictive

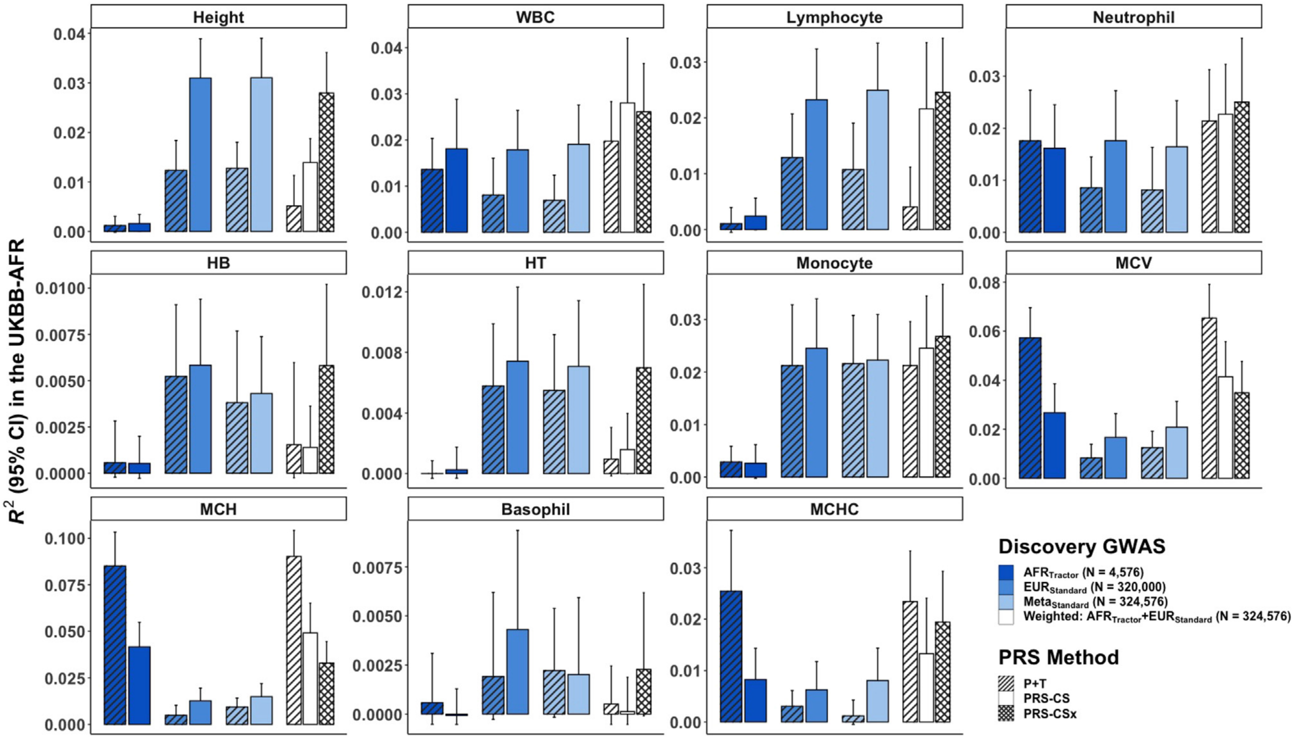

Figure 6. Accuracy of PRSs derived from local ancestry-informed GWASs vs. other discovery GWASs in the UKBB-AFR population

$AFR_{Tractor}$ denotes the AFR-specific GWAS performed using Tractor on the UKBB admixed AFR-EUR individuals. $EUR_{standard}$ refers to standard GWASs performed on the EUR population in the UKBB. $Meta_{standard}$ is the meta-analysis performed on $AFR_{Tractor}$ and $EUR_{standard}$. Furthermore, we constructed a weighted PRS by combining PRSs generated from $AFR_{Tractor}$ and $EUR_{standard}$ through a linear weighted approach. The figure shows the results for traits with SNP-based heritability >0.1 in the UKBB-AFR. Full results are shown in Table S10.

accuracy of $AFR_{Tractor}$-derived PRSs for most traits such as height and BMI (Figure 6; Table S10). However, we observed notable improvements for 5 traits, including WBC, neutrophil count (neutrophil), MCV, MCH, and MCHC, where $AFR_{Tractor}$-derived PRSs achieved significantly higher R^2 compared with $EUR_{standard}$-derived PRSs when using P + T (0.040 vs. 0.007, one-sided paired t test, p = 0.038), despite a much larger sample size for $EUR_{standard}$. This improvement might be attributed to the presence of large-effect AFR-enriched variants, particularly for MCV, MCH, and MCHC, which are effectively captured by Tractor GWASs.[6,19] Consistent with our previous findings, P + T generally outperformed PRS-CS for these traits, characterized by much sparser genetic architectures, with a mean R^2 of 0.040 compared with 0.022. In line with our PRS accuracy results, we observed higher estimates of SNP-based heritability for WBC (h^2 = 0.41, SE = 0.19 vs. h^2 = 0.17, SE = 0.01), neutrophil (h^2 = 0.44, SE = 0.26 vs. h^2 = 0.15, SE = 0.01), and MCHC (h^2 = 0.15, SE = 0.11 vs. h^2 = 0.06, SE = 0.01) in the AFR population compared with in the EUR population (STAR Methods). However, these differences did not reach statistical significance, which can be attributed to the large SEs resulting from the limited small sample size of the AFR population and the sparser genetic architectures, leading to less stable heritability estimates using LDSC.

The best local ancestry-informed PRS approach that we evaluated for the 5 less polygenic traits was $PRS_{weighted}$. This finding aligns with our earlier observations, where $PRS_{weighted}$ outperformed PRS_{multi} for traits with large-effect ancestry-enriched variants, while PRS_{multi} exhibited superior overall performance for traits lacking such variants. Specifically, the mean accuracies of $PRS_{weighted}$ using P + T, PRS-CS, and PRS-CSx for those 5 traits were 0.044, 0.031, and 0.028, respectively, with no significant differences observed among the three PRS methods. The mean accuracies of $Meta_{standard}$-derived PRSs were 0.016 and 0.008 using PRS-CS and P + T, respectively. Additionally, we did not observe significant accuracy differences between PRSs derived from GWASs conducted using standard linear regression in admixed populations and $AFR_{Tractor}$-derived PRSs (Table S10). It is worth noting that the effective sample size of local ancestry-informed GWASs is approximately 20% smaller due to the reduction from deconvolving ancestral tracts. Moreover, PRSs derived from traditional GWASs in admixed populations necessitate an in-sample LD reference panel. In contrast, local ancestry-informed GWAS-based PRSs, as shown in this study, can leverage external LD reference panels, eliminating the need for direct access to individual-level genotypes of admixed populations.

DISCUSSION

In this study, we extensively evaluated PRS performance through a combination of simulation and empirical analyses to explore the impact of various factors on PRS predictive accuracy

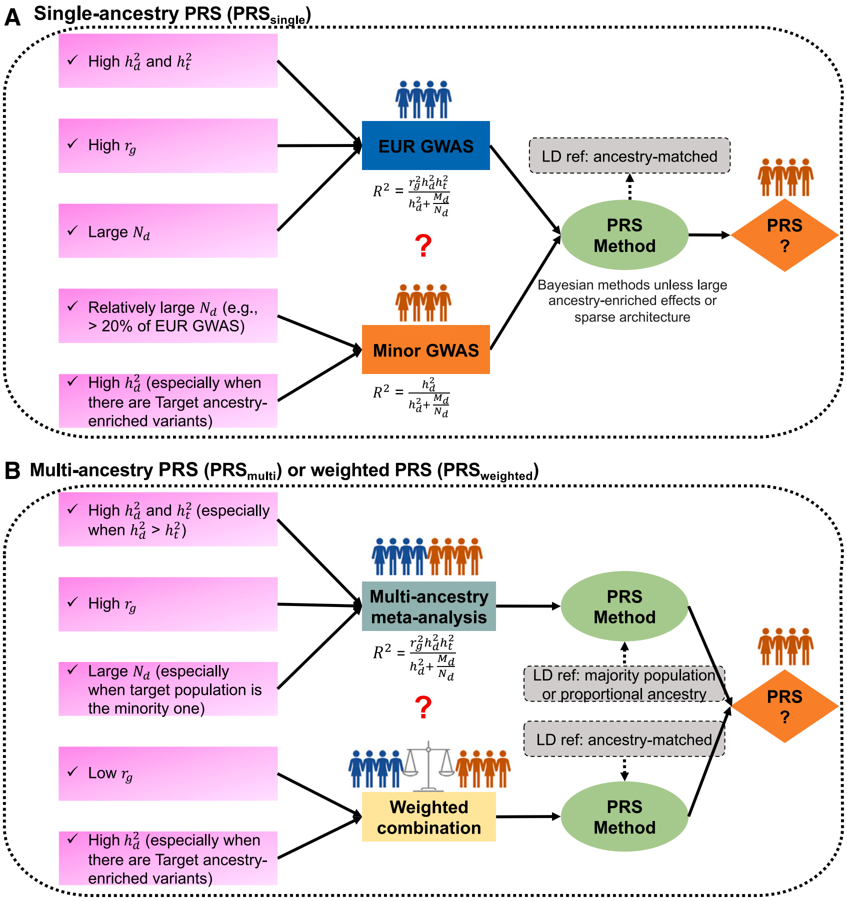
A Single-ancestry PRS (PRS$_{single}$)
✓ High h_d^2 and h_t^2
✓ High r_g
✓ Large N_d
✓ Relatively large N_d (e.g., > 20% of EUR GWAS)
✓ High h_d^2 (especially when there are Target ancestry-enriched variants)
EUR GWAS
$R^2 = \frac{r_g^2 h_d^2 h_t^2}{h_d^2 + \frac{M_d}{N_d}}$
?
Minor GWAS
$R^2 = \frac{h_d^2}{h_d^2 + \frac{M_d}{N_d}}$
LD ref: ancestry-matched
PRS Method
Bayesian methods unless large ancestry-enriched effects or sparse architecture
PRS ?
B Multi-ancestry PRS (PRS$_{multi}$) or weighted PRS (PRS$_{weighted}$)
✓ High h_d^2 and h_t^2 (especially when h_d^2 > h_t^2)
✓ High r_g
✓ Large N_d (especially when target population is the minority one)
✓ Low r_g
✓ High h_d^2 (especially when there are Target ancestry-enriched variants)
Multi-ancestry meta-analysis
$R^2 = \frac{r_g^2 h_d^2 h_t^2}{h_d^2 + \frac{M_d}{N_d}}$
?
Weighted combination
PRS Method
LD ref: majority population or proportional ancestry
LD ref: ancestry-matched
PRS Method
PRS ?

Figure 7. General practices for developing PRSs using different discovery GWASs

We summarized the general practice for developing PRSs (A) using single-ancestry GWASs (PRS$_{single}$) and (B) using GWASs from multiple ancestries (PRS$_{multi}$ or PRS$_{weighted}$). r_g, cross-ancestry genetic correlation; h_d^2 and h_t^2, SNP-based heritability in discovery and target populations, respectively; N_d, discovery GWAS sample size; M_d, the number of genome-wide independent segments in the discovery population.

and generalizability across populations. We demonstrated that increasing genetic diversity of discovery GWASs improved predictive accuracy in understudied populations. The extent of improvement was influenced by factors such as sample size ratios between EUR GWASs and Minor GWASs, genetic architecture, PRS methodology, and LD reference panels. Among those factors, between-ancestry genetic architecture differences, such as ancestry-enriched variants with large effects, affected accuracy improvement more than other factors. While leveraging large-scale EUR GWASs continues to benefit PRS accuracy given the current scale of understudied populations, we may not expect accuracy improvement when meta-analyzing extremely small Minor GWASs.[6]

Our study also revealed that directly meta-analyzing datasets from diverse ancestral groups could yield greater accuracy improvements than linearly combining PRSs through an optimized weighting strategy, especially for P + T. Such improvements from meta-analyzed GWASs support the common implicit assumption that causal variants are shared between ancestries. Consistent with this assumption, when smaller target populations lack representation, leveraging genetic information from a different population with larger sample sizes improves PRS accuracy, even when it is ancestrally diverged. Notably, when employing the more sophisticated genome-wide PRS method, PRS-CSx, accuracy differences between PRS$_{multi}$ and PRS$_{weighted}$ were marginal. Moreover, PRS-CSx generally outperformed PRS-CS, with the exception of BMI. The improvement was most pronounced for traits with ancestry-specific variants, such as MCV and MCH.

We have comprehensively evaluated characteristics that impact PRS performance, including in recently admixed populations. We have shown the advantage of leveraging GWASs in admixed populations by accounting for local ancestry, which could improve PRS predictive performance in understudied populations even without direct access to individual genotypes of admixed populations. Specifically, we found that PRS$_{weighted}$ consistently outperformed PRS$_{multi}$ for traits with ancestry-enriched variants. However, the sample size of admixed individuals here was relatively small, and we anticipate that future analyses incorporating larger datasets, such as the All of Us Research Program, will provide further insights into optimal PRS strategies for improved accuracy and generalizability using PRSs derived from local ancestry-informed GWASs.

While previous studies have shown the advantages of leveraging increased genetic diversity to improve PRS accuracy in global populations,[7,35] most have used GWASs with primarily EUR ancestry. Here, we have provided additional best practices for developing PRSs for understudied populations using diverse discovery cohorts, particularly when GWASs encompass different ancestry compositions across various trait genetic architectures (Figure 7). Our recommendations primarily revolve around general guidelines for constructing PRS$_{single}$ and PRS$_{multi}$ (or PRS$_{weighted}$), depending on factors examined in this study (Figure S13).

First, in the development of PRS$_{single}$, we employed a theoretical equation[36] to enhance the selection of input GWASs (STAR Methods), as a function of r_g, SNP-based heritability in discovery and target populations, GWAS sample size, and the number of genome-wide independent segments in the discovery population.[36] For traits with relatively low r_g and a sizable ancestry-matched GWAS (e.g., >20%–40% of EUR GWASs), such as BMI and height, PRS accuracy in the target population improves when ancestry-matched GWASs are utilized. On the other hand, for traits with high r_g and high SNP-based heritability, we expect larger-scale EUR GWASs to outperform smaller-scale ancestry-matched GWASs. Additionally, we expect Bayesian methods tailored to trait-specific genetic architecture to outperform P + T. However, this superior performance may not hold true for traits that exhibit large-effect ancestry-enriched variants or with a very sparse genetic architecture, which are attributes typically informed by prior knowledge or information gleaned from literature and public resources.[35,37–39] To enhance accuracy in such scenarios, we recommend employing a grid-search approach with a finer-scale adjustment of the hyper-parameters in Bayesian methods.

Second, in comparison to $\text{PRS}_{\text{single}}$ derived from large-scale EUR GWASs, we recommend using $\text{PRS}_{\text{multi}}$, unless the target ancestry-matched GWAS is extremely small (<10,000). $\text{PRS}_{\text{multi}}$ is generally preferred for traits with high r_g, high SNP-based heritability, and large sample sizes. We find increasing evidence supporting the notion that the effects of most common variants are shared between ancestries, indicating a high r_g for most traits.[9,11] However, estimates of r_g can be affected by phenotypic and environmental heterogeneity across populations.[10,16] When constructing $\text{PRS}_{\text{multi}}$ using summary-level-based methods, researchers should carefully consider which LD reference panel best approximates the LD structure between SNPs while being the most readily accessible. We have shown that when EUR remains the majority population in the discovery GWAS, using the EUR-based reference panel effectively approximates the LD of the discovery GWAS, consistent with our previous findings.[7]

Third, our findings indicate the advantages of $\text{PRS}_{\text{multi}}$ compared with $\text{PRS}_{\text{weighted}}$, particularly when employing P + T and PRS-CS. However, there are some notable exceptions, such as the higher accuracy observed when using $\text{PRS}_{\text{weighted}}$ with PRS-CS for traits with low r_g, such as height. Furthermore, when incorporating local ancestry-informed GWASs and large-scale EUR GWASs, $\text{PRS}_{\text{weighted}}$ outperformed $\text{PRS}_{\text{multi}}$ for traits with AFR-enriched variants, such as WBC and MCHC, in the UKBB-AFR. On the other hand, we note that the accuracy of $\text{PRS}_{\text{multi}}$ could be more affected by the choice of LD reference panel, while $\text{PRS}_{\text{weighted}}$ was not limited in this regard due to its easy accessibility of external ancestry-matched reference panels. PRS-CSx is recommended when ancestry-specific GWASs from multiple populations are available, especially with considerable sample sizes (e.g., >25,000–50,000) of Minor GWASs. These results highlight the importance of making ancestry-specific summary statistics publicly available.

In summary, there is no one-size-fits all approach for constructing PRSs, as the optimal approach depends on genetic architecture, ancestry composition, statistical power, and other factors. These factors can be complex, particularly as a deluge of methods are being developed to address the PRS generalizability problem. To inform optimal approaches across a wide range of scenarios, we have distilled the results of extensive simulations and empirical analyses across trait genetic architectures, ancestries, and methods into a set of guidelines from parameters that are typically evaluated at the outset of a genetic study.

Limitations of the study

We acknowledge some limitations and future directions in our study. First, we focused on common variants, while population-enriched variants have lower frequencies in the overall population. The role of such variants in polygenic prediction are worth exploring across phenotypes when there are sufficient sample sizes for different ancestral populations. Second, as we used external LD reference panels for PRS construction, PRS performance decreases with LD mismatch between the discovery population and the LD reference panel, especially when using multi-ancestry GWASs. While we show that LD reference panel differences have a relatively modest effect on PRS accuracy, they have a much larger effect on fine-mapping,[40] so future efforts are warranted to share in-sample LD without direct access to individual-level genotypes, especially for large consortia with numerous and diverse cohorts. Alternatively, developing more sophisticated individual-level PRS methods that preserve privacy and are scalable to current biobank-scale data is also promising. Third, while our primary focus pertains to quantitative phenotypes characterized by diverse genetic architectures, we expect that our findings can be broadly applied to binary traits, as we have investigated previously.[7] However, binary phenotypes introduce additional complexities due to factors such as variable case/control ratios, phenotype definitions, environmental differences, and smaller effective sample sizes or lower statistical power. Finally, it is important to acknowledge that our study focused on selected methods, which consistently exhibit similar trends. Although we anticipate that our findings are broadly applicable to alternative methods, such as XPASS[41] and XP-BLUP,[42] further research is needed to explore the generalizability of our findings to other polygenic prediction approaches. Despite the limitations, our study highlights the advantages of leveraging the increasing diversity of current genomics studies to improve polygenic prediction across populations. We emphasize the necessity of diversifying not only the ancestry but also the phenotypic spectrum when collecting genomic data from global populations, which will contribute to achieve a more equitable and effective use of PRSs for traits with varying genetic architectures.

STAR★METHODS

Detailed methods are provided in the online version of this paper and include the following:

- KEY RESOURCES TABLE
- RESOURCE AVAILABILITY
  - ○ Lead contact
  - ○ Materials availability
  - ○ Data and code availability
- METHOD DETAILS
  - ○ Simulations
  - ○ Simulated phenotypes with varying trait genetic architecture
  - ○ Downsampling and meta-analyzed GWAS in simulations
  - ○ Pruning and thresholding (P + T) in simulations
  - ○ Empirical analysis of 17 quantitative traits in the UK biobank (UKBB) and biobank Japan (BBJ)
  - ○ Datasets and quality control (QC)
  - ○ PRS construction for 17 traits in empirical analysis
  - ○ UK biobank recent admixture ancestry analysis

SUPPLEMENTAL INFORMATION

Supplemental information can be found online at https://doi.org/10.1016/j.xgen.2023.100408.

ACKNOWLEDGMENTS

A.R.M. and Y.W. are supported by NIH (K99/R00MH117229 to A.R.M.) and by the European Union's Horizon 2020 research and innovation program under grant agreement 101016775. A.R.M. is also supported by U01HG011719. H.H. acknowledges support from NIDDK K01DK114379, NIDDK 1R01DK129364, NIMH U01MH109539, the Zhengxu and Ying He Foundation, and the Stanley Center for Psychiatric Research. E.G.A. is supported by K01MH121659 from NIMH, the Caroline Wiess Law Fund for Research in Molecular Medicine, and the ARCO Foundation Young Teacher-Investigator Fund at Baylor College of Medicine. P.T. is supported by NIH/NIA (R00 AG062787) and by the Good Ventures Foundation (010623-00001).

AUTHOR CONTRIBUTIONS

Conceptualization, Y.W., A.R.M., E.G.A., and M. Kanai; formal analysis, Y.W., M. Kanai., T.T., M. Kamariza., K.Y., W.Z., and P.T.; writing – original draft, Y.W., A.R.M., E.G.A., M. Kanai., and T.T.; writing – review & editing, Y.W., M. Kanai., T.T., M. Kamariza, K.T., K.Y., W.Z., Y.O., H.H., P.T., E.G.A., and A.R.M.

DECLARATION OF INTERESTS

H.H. received consultancy fees from Ono Pharmaceutical and honorarium from Xian Janssen Pharmaceutical.

Received: January 31, 2023
Revised: June 21, 2023
Accepted: August 22, 2023
Published: September 14, 2023

REFERENCES

1. Inouye, M., Abraham, G., Nelson, C.P., Wood, A.M., Sweeting, M.J., Dudbridge, F., Lai, F.Y., Kaptoge, S., Brozynska, M., Wang, T., et al. (2018). Genomic Risk Prediction of Coronary Artery Disease in 480,000 Adults: Implications for Primary Prevention. J. Am. Coll. Cardiol. *72*, 1883–1893. https://doi.org/10.1016/j.jacc.2018.07.079.
2. Khera, A.V., Chaffin, M., Aragam, K.G., Haas, M.E., Roselli, C., Choi, S.H., Natarajan, P., Lander, E.S., Lubitz, S.A., Ellinor, P.T., and Kathiresan, S. (2018). Genome-wide polygenic scores for common diseases identify individuals with risk equivalent to monogenic mutations. Nat. Genet. *50*, 1219–1224. https://doi.org/10.1038/s41588-018-0183-z.
3. Mars, N., Widén, E., Kerminen, S., Meretoja, T., Pirinen, M., Della Briotta Parolo, P., Palta, P., FinnGen; Palotie, A., Kaprio, J., et al. (2020). The role of polygenic risk and susceptibility genes in breast cancer over the course of life. Nat. Commun. *11*, 6383. https://doi.org/10.1038/s41467-020-19966-5.
4. Maas, P., Barrdahl, M., Joshi, A.D., Auer, P.L., Gaudet, M.M., Milne, R.L., Schumacher, F.R., Anderson, W.F., Check, D., Chattopadhyay, S., et al. (2016). Breast Cancer Risk From Modifiable and Nonmodifiable Risk Factors Among White Women in the United States. JAMA Oncol. *2*, 1295–1302. https://doi.org/10.1001/jamaoncol.2016.1025.
5. Craig, J.E., Han, X., Qassim, A., Hassall, M., Cooke Bailey, J.N., Kinzy, T.G., Khawaja, A.P., An, J., Marshall, H., Gharahkhani, P., et al. (2020). Multitrait analysis of glaucoma identifies new risk loci and enables polygenic prediction of disease susceptibility and progression. Nat. Genet. *52*, 160–166. https://doi.org/10.1038/s41588-019-0556-y.
6. Majara, L., Kalungi, A., Koen, N., Tsuo, K., Wang, Y., Gupta, R., Nkambule, L.L., Zar, H., Stein, D.J., Kinyanda, E., et al. (2023). Low and differential polygenic score generalizability among African populations due largely to genetic diversity. HGG Adv. *4*, 100184. https://doi.org/10.1016/j.xhgg.2023.100184.
7. Wang, Y., Namba, S., Lopera, E., Kerminen, S., Tsuo, K., Läll, K., Kanai, M., Zhou, W., Wu, K.-H., Favé, M.J., et al. (2023). Global Biobank analyses provide lessons for developing polygenic risk scores across diverse cohorts. Cell Genom. *3*, 100241. https://doi.org/10.1016/j.xgen.2022.100241.
8. Ruan, Y., Lin, Y.-F., Feng, Y.-C.A., Chen, C.-Y., Lam, M., Guo, Z., Stanley Global Asia Initiatives; He, L., Sawa, A., Martin, A.R., et al. (2022). Improving polygenic prediction in ancestrally diverse populations. Nat. Genet. *54*, 573–580. https://doi.org/10.1038/s41588-022-01054-7.
9. Wang, Y., Guo, J., Ni, G., Yang, J., Visscher, P.M., and Yengo, L. (2020). Theoretical and empirical quantification of the accuracy of polygenic scores in ancestry divergent populations. Nat. Commun. *11*, 3865. https://doi.org/10.1038/s41467-020-17719-y.
10. Guo, J., Bakshi, A., Wang, Y., Jiang, L., Yengo, L., Goddard, M.E., Visscher, P.M., and Yang, J. (2021). Quantifying genetic heterogeneity between continental populations for human height and body mass index. Sci. Rep. *11*, 5240. https://doi.org/10.1038/s41598-021-84739-z.
11. Shi, H., Burch, K.S., Johnson, R., Freund, M.K., Kichaev, G., Mancuso, N., Manuel, A.M., Dong, N., and Pasaniuc, B. (2020). Localizing Components of Shared Transethnic Genetic Architecture of Complex Traits from GWAS Summary Data. Am. J. Hum. Genet. *106*, 805–817. https://doi.org/10.1016/j.ajhg.2020.04.012.
12. Ding, Y., Hou, K., Xu, Z., Pimplaskar, A., Petter, E., Boulier, K., Privé, F., Vilhjálmsson, B.J., Olde Loohuis, L.M., and Pasaniuc, B. (2023). Polygenic scoring accuracy varies across the genetic ancestry continuum. Nature *618*, 774–781. https://doi.org/10.1038/s41586-023-06079-4.
13. Pfaff, C.L., Parra, E.J., Bonilla, C., Hiester, K., McKeigue, P.M., Kamboh, M.I., Hutchinson, R.G., Ferrell, R.E., Boerwinkle, E., and Shriver, M.D. (2001). Population structure in admixed populations: effect of admixture dynamics on the pattern of linkage disequilibrium. Am. J. Hum. Genet. *68*, 198–207. https://doi.org/10.1086/316935.
14. Pritchard, J.K., and Przeworski, M. (2001). Linkage disequilibrium in humans: models and data. Am. J. Hum. Genet. *69*, 1–14. https://doi.org/10.1086/321275.
15. Fatumo, S., Chikowore, T., Choudhury, A., Ayub, M., Martin, A.R., and Kuchenbaecker, K. (2022). A roadmap to increase diversity in genomic studies. Nat. Med. *28*, 243–250. https://doi.org/10.1038/s41591-021-01672-4.
16. Hou, K., Ding, Y., Xu, Z., Wu, Y., Bhattacharya, A., Mester, R., Belbin, G.M., Buyske, S., Conti, D.V., Darst, B.F., et al. (2023). Causal effects on complex traits are similar for common variants across segments of different continental ancestries within admixed individuals. Nat. Genet. *55*, 549–558. https://doi.org/10.1038/s41588-023-01338-6.
17. Kim, J., Edge, M.D., Goldberg, A., and Rosenberg, N.A. (2021). Skin deep: The decoupling of genetic admixture levels from phenotypes that differed between source populations. Am. J. Phys. Anthropol. *175*, 406–421. https://doi.org/10.1002/ajpa.24261.
18. Maples, B.K., Gravel, S., Kenny, E.E., and Bustamante, C.D. (2013). RFMix: a discriminative modeling approach for rapid and robust local-ancestry inference. Am. J. Hum. Genet. *93*, 278–288. https://doi.org/10.1016/j.ajhg.2013.06.020.
19. Atkinson, E.G., Maihofer, A.X., Kanai, M., Martin, A.R., Karczewski, K.J., Santoro, M.L., Ulirsch, J.C., Kamatani, Y., Okada, Y., Finucane, H.K., et al. (2021). Tractor uses local ancestry to enable the inclusion of admixed individuals in GWAS and to boost power. Nat. Genet. *53*, 195–204. https://doi.org/10.1038/s41588-020-00766-y.
20. Pasaniuc, B., Zaitlen, N., Lettre, G., Chen, G.K., Tandon, A., Kao, W.H.L., Ruczinski, I., Fornage, M., Siscovick, D.S., Zhu, X., et al. (2011). Enhanced statistical tests for GWAS in admixed populations: assessment using African Americans from CARe and a Breast Cancer Consortium. PLoS Genet. *7*, e1001371. https://doi.org/10.1371/journal.pgen.1001371.

21. Ramirez, A.H., Sulieman, L., Schlueter, D.J., Halvorson, A., Qian, J., Ratsimbazafy, F., Loperena, R., Mayo, K., Basford, M., Deflaux, N., et al. (2022). The All of Us Research Program: Data quality, utility, and diversity. Patterns (N Y) *3*, 100570. https://doi.org/10.1016/j.patter.2022.100570.

22. Weissbrod, O., Kanai, M., Shi, H., Gazal, S., Peyrot, W.J., Khera, A.V., Okada, Y., Biobank Japan Project; Martin, A.R., Finucane, H.K., and Price, A.L. (2022). Leveraging fine-mapping and multipopulation training data to improve cross-population polygenic risk scores. Nat. Genet. *54*, 450–458. https://doi.org/10.1038/s41588-022-01036-9.

23. Zhang, H., Zhan, J., Jin, J., Ahearn, T.U., Yu, Z., O'Connell, J., Jiang, Y., Chen, T., Garcia-Closas, M., Lin, X., et al. (2022). Novel Methods for Multi-ancestry Polygenic Prediction and their Evaluations in 3.7 Million Individuals of Diverse Ancestry. Preprint at bioRxiv. https://doi.org/10.1101/2022.03.24.485519.

24. Wray, N.R., Yang, J., Hayes, B.J., Price, A.L., Goddard, M.E., and Visscher, P.M. (2013). Pitfalls of predicting complex traits from SNPs. Nat. Rev. Genet. *14*, 507–515. https://doi.org/10.1038/nrg3457.

25. Daetwyler, H.D., Villanueva, B., and Woolliams, J.A. (2008). Accuracy of predicting the genetic risk of disease using a genome-wide approach. PLoS One *3*, e3395. https://doi.org/10.1371/journal.pone.0003395.

26. Nagai, A., Hirata, M., Kamatani, Y., Muto, K., Matsuda, K., Kiyohara, Y., Ninomiya, T., Tamakoshi, A., Yamagata, Z., Mushiroda, T., et al. (2017). Overview of the BioBank Japan Project: Study design and profile. J. Epidemiol. *27*, S2–S8. https://doi.org/10.1016/j.je.2016.12.005.

27. Bycroft, C., Freeman, C., Petkova, D., Band, G., Elliott, L.T., Sharp, K., Motyer, A., Vukcevic, D., Delaneau, O., O'Connell, J., et al. (2018). The UK Biobank resource with deep phenotyping and genomic data. Nature *562*, 203–209. https://doi.org/10.1038/s41586-018-0579-z.

28. Morales, J., Welter, D., Bowler, E.H., Cerezo, M., Harris, L.W., McMahon, A.C., Hall, P., Junkins, H.A., Milano, A., Hastings, E., et al. (2018). A standardized framework for representation of ancestry data in genomics studies, with application to the NHGRI-EBI GWAS Catalog. Genome Biol. *19*, 21. https://doi.org/10.1186/s13059-018-1396-2.

29. Zeng, J., Xue, A., Jiang, L., Lloyd-Jones, L.R., Wu, Y., Wang, H., Zheng, Z., Yengo, L., Kemper, K.E., Goddard, M.E., et al. (2021). Widespread signatures of natural selection across human complex traits and functional genomic categories. Nat. Commun. *12*, 1164. https://doi.org/10.1038/s41467-021-21446-3.

30. Berg, J.J., Harpak, A., Sinnott-Armstrong, N., Joergensen, A.M., Mostafavi, H., Field, Y., Boyle, E.A., Zhang, X., Racimo, F., Pritchard, J.K., and Coop, G. (2019). Reduced signal for polygenic adaptation of height in UK Biobank. Elife *8*, e39725. https://doi.org/10.7554/eLife.39725.

31. Sohail, M., Maier, R.M., Ganna, A., Bloemendal, A., Martin, A.R., Turchin, M.C., Chiang, C.W., Hirschhorn, J., Daly, M.J., Patterson, N., et al. (2019). Polygenic adaptation on height is overestimated due to uncorrected stratification in genome-wide association studies. Elife *8*, e39702. https://doi.org/10.7554/eLife.39702.

32. Martin, A.R., Kanai, M., Kamatani, Y., Okada, Y., Neale, B.M., and Daly, M.J. (2019). Clinical use of current polygenic risk scores may exacerbate health disparities. Nat. Genet. *51*, 584–591. https://doi.org/10.1038/s41588-019-0379-x.

33. Lehmann, B., Mackintosh, M., McVean, G., and Holmes, C. (2023). Optimal strategies for learning multi-ancestry polygenic scores vary across traits. Nat. Commun. *14*, 4023. https://doi.org/10.1038/s41467-023-38930-7.

34. Márquez-Luna, C., Loh, P.-R., and A.LSIGMA Type 2 Diabetes Consortium, Price; South Asian Type 2 Diabetes SAT2D Consortium. (2017). Multiethnic polygenic risk scores improve risk prediction in diverse populations. Genet. Epidemiol. *41*, 811–823. https://doi.org/10.1002/gepi.22083.

35. Graham, S.E., Clarke, S.L., Wu, K.-H.H., Kanoni, S., Zajac, G.J.M., Ramdas, S., Surakka, I., Ntalla, I., Vedantam, S., Winkler, T.W., et al. (2021). The power of genetic diversity in genome-wide association studies of lipids. Nature *600*, 675–679. https://doi.org/10.1038/s41586-021-04064-3.

36. de Vlaming, R., Okbay, A., Rietveld, C.A., Johannesson, M., Magnusson, P.K.E., Uitterlinden, A.G., van Rooij, F.J.A., Hofman, A., Groenen, P.J.F., Thurik, A.R., and Koellinger, P.D. (2017). Meta-GWAS Accuracy and Power (MetaGAP) Calculator Shows that Hiding Heritability Is Partially Due to Imperfect Genetic Correlations across Studies. PLoS Genet. *13*, e1006495. https://doi.org/10.1371/journal.pgen.1006495.

37. Ni, G., Zeng, J., Revez, J.A., Wang, Y., Zheng, Z., Ge, T., Restuadi, R., Kiewa, J., Nyholt, D.R., Coleman, J.R.I., et al. (2021). A Comparison of Ten Polygenic Score Methods for Psychiatric Disorders Applied Across Multiple Cohorts. Biol. Psychiatr. *90*, 611–620. https://doi.org/10.1016/j.biopsych.2021.04.018.

38. Lloyd-Jones, L.R., Zeng, J., Sidorenko, J., Yengo, L., Moser, G., Kemper, K.E., Wang, H., Zheng, Z., Magi, R., Esko, T., et al. (2019). Improved polygenic prediction by Bayesian multiple regression on summary statistics. Nat. Commun. *10*, 5086. https://doi.org/10.1038/s41467-019-12653-0.

39. Ge, T., Chen, C.-Y., Ni, Y., Feng, Y.-C.A., and Smoller, J.W. (2019). Polygenic prediction via Bayesian regression and continuous shrinkage priors. Nat. Commun. *10*, 1776. https://doi.org/10.1038/s41467-019-09718-5.

40. Daly, M.J., Elzur, R., Global Biobank Meta-analysis Initiative; Zhou, W., Kanai, M., Finucane, H.K., Rasheed, H., Tsuo, K., Hirbo, J.B., Wang, Y., et al. (2022). Meta-analysis fine-mapping is often miscalibrated at single-variant resolution. Cell Genom. *2*, 100210. https://doi.org/10.1016/j.xgen.2022.100210.

41. Cai, M., Xiao, J., Zhang, S., Wan, X., Zhao, H., Chen, G., and Yang, C. (2021). A unified framework for cross-population trait prediction by leveraging the genetic correlation of polygenic traits. Am. J. Hum. Genet. *108*, 632–655. https://doi.org/10.1016/j.ajhg.2021.03.002.

42. Coram, M.A., Fang, H., Candille, S.I., Assimes, T.L., and Tang, H. (2017). Leveraging Multi-ethnic Evidence for Risk Assessment of Quantitative Traits in Minority Populations. Am. J. Hum. Genet. *101*, 218–226. https://doi.org/10.1016/j.ajhg.2017.06.015.

43. 1000 Genomes Project Consortium; Auton, A., Brooks, L.D., Durbin, R.M., Garrison, E.P., Kang, H.M., Korbel, J.O., Marchini, J.L., McCarthy, S., McVean, G.A., and Abecasis, G.R. (2015). A global reference for human genetic variation. Nature *526*, 68–74. https://doi.org/10.1038/nature15393.

44. Chang, C.C., Chow, C.C., Tellier, L.C., Vattikuti, S., Purcell, S.M., and Lee, J.J. (2015). Second-generation PLINK: rising to the challenge of larger and richer datasets. GigaScience *4*, 7. https://doi.org/10.1186/s13742-015-0047-8.

45. Su, Z., Marchini, J., and Donnelly, P. (2011). HAPGEN2: simulation of multiple disease SNPs. Bioinformatics *27*, 2304–2305. https://doi.org/10.1093/bioinformatics/btr341.

46. Manichaikul, A., Mychaleckyj, J.C., Rich, S.S., Daly, K., Sale, M., and Chen, W.-M. (2010). Robust relationship inference in genome-wide association studies. Bioinformatics *26*, 2867–2873. https://doi.org/10.1093/bioinformatics/btq559.

47. Willer, C.J., Li, Y., and Abecasis, G.R. (2010). METAL: fast and efficient meta-analysis of genomewide association scans. Bioinformatics *26*, 2190–2191. https://doi.org/10.1093/bioinformatics/btq340.

48. Li, J.Z., Absher, D.M., Tang, H., Southwick, A.M., Casto, A.M., Ramachandran, S., Cann, H.M., Barsh, G.S., Feldman, M., Cavalli-Sforza, L.L., and Myers, R.M. (2008). Worldwide human relationships inferred from genome-wide patterns of variation. Science *319*, 1100–1104. https://doi.org/10.1126/science.1153717.

49. Conomos, M.P., Reiner, A.P., Weir, B.S., and Thornton, T.A. (2016). Model-free Estimation of Recent Genetic Relatedness. Am. J. Hum. Genet. *98*, 127–148. https://doi.org/10.1016/j.ajhg.2015.11.022.

50. Loh, P.-R., Palamara, P.F., and Price, A.L. (2016). Fast and accurate long-range phasing in a UK Biobank cohort. Nat. Genet. *48*, 811–816. https://doi.org/10.1038/ng.3571.

51. Das, S., Forer, L., Schönherr, S., Sidore, C., Locke, A.E., Kwong, A., Vrieze, S.I., Chew, E.Y., Levy, S., McGue, M., et al. (2016). Next-generation

genotype imputation service and methods. Nat. Genet. *48*, 1284–1287. https://doi.org/10.1038/ng.3656.

52. Akiyama, M., Ishigaki, K., Sakaue, S., Momozawa, Y., Horikoshi, M., Hirata, M., Matsuda, K., Ikegawa, S., Takahashi, A., Kanai, M., et al. (2019). Characterizing rare and low-frequency height-associated variants in the Japanese population. Nat. Commun. *10*, 4393. https://doi.org/10.1038/s41467-019-12276-5.

53. Sakaue, S., Kanai, M., Tanigawa, Y., Karjalainen, J., Kurki, M., Koshiba, S., Narita, A., Konuma, T., Yamamoto, K., Akiyama, M., et al. (2021). A cross-population atlas of genetic associations for 220 human phenotypes. Nat. Genet. *53*, 1415–1424. https://doi.org/10.1038/s41588-021-00931-x.

54. Kanai, M., Akiyama, M., Takahashi, A., Matoba, N., Momozawa, Y., Ikeda, M., Iwata, N., Ikegawa, S., Hirata, M., Matsuda, K., et al. (2018). Genetic analysis of quantitative traits in the Japanese population links cell types to complex human diseases. Nat. Genet. *50*, 390–400. https://doi.org/10.1038/s41588-018-0047-6.

55. Wray, N.R., Kemper, K.E., Hayes, B.J., Goddard, M.E., and Visscher, P.M. (2019). Complex Trait Prediction from Genome Data: Contrasting EBV in Livestock to PRS in Humans: Genomic Prediction. Genetics *211*, 1131–1141. https://doi.org/10.1534/genetics.119.301859.

56. International HapMap 3 Consortium; Altshuler, D.M., Gibbs, R.A., Peltonen, L., Altshuler, D.M., Gibbs, R.A., Peltonen, L., Dermitzakis, E., Schaffner, S.F., Yu, F., et al. (2010). Integrating common and rare genetic variation in diverse human populations. Nature *467*, 52–58. https://doi.org/10.1038/nature09298.

57. Privé, F., Vilhjálmsson, B.J., Aschard, H., and Blum, M.G.B. (2019). Making the Most of Clumping and Thresholding for Polygenic Scores. Am. J. Hum. Genet. *105*, 1213–1221. https://doi.org/10.1016/j.ajhg.2019.11.001.

STAR★METHODS

KEY RESOURCES TABLE

REAGENT or RESOURCE	SOURCE	IDENTIFIER
Deposited data		
1000 Genome Phase 3	[43]	ftp://ftp.1000genomes.ebi.ac.uk/vol1/ftp/data_collections/1000_genomes_project/data
Software and algorithms		
Plink	[44]	https://www.cog-genomics.org/plink/
PRS-CS	[39]	https://github.com/getian107/PRScs
SBayesS/GCTB	[29]	https://cnsgenomics.com/software/gctb/
PRS-CSx	[8]	https://github.com/getian107/PRScsx
Tractor	[19]	https://github.com/Atkinson-Lab/Tractor
HapGen2	[45]	https://mathgen.stats.ox.ac.uk/genetics_software/hapgen/hapgen2.html
Codes for this study	This paper	https://doi.org/10.5281/zenodo.8218174

RESOURCE AVAILABILITY

Lead contact

Further information and requests for resources and reagents should be directed to and will be fulfilled by the lead contact, Ying Wang (yiwang@broadinstitute.org).

Materials availability

This study did not generate new unique reagents.

Data and code availability

1000 Genome Phase 3 data can be accessed at ftp://ftp.1000genomes.ebi.ac.uk/vol1/ftp/data_collections/1000_genomes_project/data. We used UK Biobank data via application 31063. The software used in this study can be found at: Plink (https://www.cog-genomics.org/plink/), PRS-CS (https://github.com/getian107/PRScs), PRS-CSx (https://github.com/getian107/PRScsx), Tractor (https://github.com/Atkinson-Lab/Tractor), HapGen2 (https://mathgen.stats.ox.ac.uk/genetics_software/hapgen/hapgen2.html) and SBayesS/GCTB (https://cnsgenomics.com/software/gctb/). The Pan UK Biobank Project can be accessed at: Pan-UK Biobank Project https://pan.ukbb.broadinstitute.org. The codes used in this study have been deposited to https://doi.org/10.5281/zenodo.8218174.

METHOD DETAILS

Simulations

Simulated genotypes in three populations

To explore the potential improvement of predictive accuracy within an underrepresented target ancestry through the inclusion of additional samples included in the multi-ancestry discovery GWAS, we simulated genotypes of chromosome 22 for 560,000 individuals in each population including European ancestry (EUR), East Asian ancestry (EAS) and African ancestry (AFR) using the software HapGen2 v2.1.2.[45] We used the haplotypes from 1000 Genome Project (1KG, Phase 3)[43] as the sample pool. We excluded Americans of African Ancestry in SW USA and African Caribbeans in Barbados from the AFR samples due to their high degree of recent admixture. We used default parameters in HapGen2 with effective sample sizes of 11,375, 12,239 and 17,380 for EUR, EAS and AFR, respectively.[45] After simulating the genotypes on chromosome 22, we ran analyses with a total of 87,938 overlapping SNPs across the three ancestries which passed quality control filters: minor allele frequency (MAF) > 0.01, Hardy-Weinberg Equilibrium (HWE) p value > 10^{-6} and genotype missingness rates across individuals <0.05. We then removed 2nd-degree related individuals using the software KING,[46] resulting in 534,352, 533,996 and 537,498 unrelated individuals from EUR, EAS and AFR, separately. We randomly sampled 10,000 and 520,000 individuals from each ancestry as the withheld target population and discovery population, respectively.

Simulated phenotypes with varying trait genetic architecture

For the sake of simplicity, we assumed that causal variants are shared across populations and their effect sizes are perfectly correlated (cross-ancestry genetic correlation, $r_g = 1$) in our initial simulations. The pairwise r_g among K populations is represented by a $K * K$ matrix, denoted as **R,** where the off-diagonal elements of **R** had the value of r_g and diagonal elements of **R** were set to 1. In our study, K was equal to 3, indicating the number of populations considered. We simulated phenotypes based on the simple additive model: $y = g + e$, where $g = \sum_{j=1}^{M_c} x_{ij}\beta_j$. M_c is the number of causal variants, x_{ij} is the genotype coded as 0, 1, or 2 for the j th SNP in the i th population. The effect size of j th SNP across K populations is drawn from a multivariate normal distribution, $\beta \sim MVN(0, \Sigma)$, where for the $K * K$ variance-covariance matrix, Σ, the diagonal and off-diagonal elements were $\frac{h^2}{2f_{ij}(1-f_{ij})M_c}$ and $\mathbf{R} \cdot \frac{h^2}{2f_{ij}(1-f_{ij})M_c}$, respectively. We denoted f_{ij} as the MAF of j th SNP in the i th population and h^2 as the trait heritability. We simulated the environmental effects to follow a normal distribution with 0 mean and $1 - h^2$ variance, $e \sim N(0, 1 - h^2)$. We simulated different levels of heritability for chromosome 22 ($h^2 = 0.03$ and 0.05). Additionally, we randomly sampled various numbers of causal variants (M_c = 100, 500, and 1000) from all the 87,938 SNPs. As a result, we defined a total of 6 distinct simulation scenarios that encompass a realistic spectrum of polygenicity, ranging from ~0.1% to ~1% of causal variants. To assess the impact of r_g on PRS performance, we expanded our simulation study by considering two scenarios. These scenarios aimed to capture different levels of per-variant variance explained. In scenario 1 characterized by $M_c = 100$ and $h^2 = 0.05$, the per-variant variance explained was higher. Conversely, scenario 2 involved $M_c = 1000$ and $h^2 = 0.03$, resulting in a lower per-variant variance explained. For each scenario, we varied the values of r_g to 0.6 and 0.8, respectively.

Downsampling and meta-analyzed GWAS in simulations

To provide the requisite discovery data for constructing PRS, we proceeded to perform GWAS on the simulated phenotypes. Specifically, we split the discovery population, which consisted of 520,000 unrelated individuals, into 52 evenly distributed bins, each comprising 10,000 individuals (denoted as Bin_1, Bin_2, …, $\text{Bin}_{\text{total}}$). Subsequently, we ran GWAS on each of those 52 bins independently within the three populations, using simple linear regression implemented in PLINK v2.0.[44] We excluded the causal variants when running GWAS to mimic the phenomenon of imperfect tagging. We then employed an iterative process of meta-analysis, employing the inverse-variance weighted method using METAL,[47] gradually incorporating a varying number of bins. Specifically, we commenced the meta-analysis with Bin_1+Bin_2, subsequently progressing to Bin_1+Bin_2+Bin_3, and so forth, until we encompassed the complete set of bins (Bin_1+Bin_2+Bin_3+ … +$\text{Bin}_{\text{total}}$) for each population.

To simulate a scenario resembling a meta-analysis involving multiple ancestries with varying proportions, we opted for an arbitrary selection of subsets from EUR GWAS. Specifically, we chose a range of bins, from 4 to 52 bins, with increments of 4. Subsequently, we systematically incorporated different numbers of bins, spanning from 1 to 52, from EAS and AFR populations into the EUR GWAS dataset via meta-analysis. The meta-analysis was conducted utilizing the inverse-variance weighted fixed-effects model implemented in the METAL software. This iterative process allowed us to achieve a range of sample size ratios between EUR and EAS as well as EUR and AFR, encompassing ratios from 52:1 to 4:52, in the meta-analyzed multi-ancestry GWAS (referred to as **Meta**). The simulation configuration is visually depicted in Figure 1.

Pruning and thresholding (P + T) in simulations

P + T follows a greedy heuristic algorithm wherein variants are sorted based on their p values. The algorithm iteratively descends in significance while retaining only those variants that do not exceed a predetermined LD threshold with previously retained variants. We employed PLINK v1.90 to clump quasi-independent SNPs within 500Kb windows, utilizing an LD threshold of $r^2 < 0.1$. To explore the impact of various LD reference panels on predictive accuracy of PRS, we used a total of four different LD reference panels:one for single-ancestry and three for multi-ancestry GWAS, with consideration to the ancestry composition of the discovery GWAS and the target population.

For the single-ancestry GWAS, we used an LD reference panel consisting of 10,000 individuals from the target population that were matched to the ancestry of the discovery GWAS. In the case of multi-ancestry GWAS, we used three LD reference panels. These panels included two composed of a single ancestry that did not mirror the ancestral makeup of the discovery GWAS. Specifically, one panel comprised 10,000 withheld EUR individuals, while the other panel encompassed individuals from understudied populations, either 10,000 EAS or 10,000 AFR individuals, consistent with the minority population represented in the discovery GWAS. The third LD reference panel consisted of individuals from different ancestries in proportions proportional to the discovery GWAS, amounting to a total of 10,000 samples.

We calculated PRS in the target population using 8 different p value thresholds: 5×10^{-8}, 1×10^{-6}, 1×10^{-4}, 1×10^{-3}, 0.01, 0.05, 0.1, and 1. We denoted PRS constructed from single-ancestry GWAS as single-ancestry PRS ($\text{PRS}_{\text{single}}$) and those from meta-analyzed multi-ancestry GWAS as multi-ancestry PRS ($\text{PRS}_{\text{multi}}$). We calculated the predictive accuracy as the variance explained by the PRS (R^2) through linear regression: $y \sim \text{PRS}$ and computed corresponding 95% confidence intervals (CIs) through bootstrap. To identify the optimal p value threshold associated with the highest predictive accuracy, we evenly divided the target population into a test cohort and a validation cohort. The p value threshold was optimized through a process of hyperparameter tuning in the validation cohort, and subsequently, the accuracy of the model was assessed using the test cohort. To further compare the accuracy of $\text{PRS}_{\text{multi}}$ relative to $\text{PRS}_{\text{EUR\_GWAS}}$, we calculated the relative accuracy (RA) as the difference in PRS R^2 between the PRS derived from multi-ancestry GWAS and EUR GWAS divided by the PRS R^2 in EUR ancestry from the EUR GWAS, i.e., $RA = \frac{R^2_{target}\ using\ PRS_{multi} - R^2_{target}\ using\ PRS_{EUR\_GWAS}}{R^2_{EUR}\ using\ PRS_{EUR\_GWAS}}$. Therefore, the trend of RA was consistent with the accuracy improvement of $\mathrm{PRS_{multi}}$.

Empirical analysis of 17 quantitative traits in the UK biobank (UKBB) and biobank Japan (BBJ)

We further explored how the findings from simulations generalized in real data using 17 quantitative traits shared between UKBB and BBJ, including anthropometric traits (BMI and height) and blood panel traits studied previously (Table S3).[32] The selection of these traits was motivated by their widespread availability within biobanks and their substantial statistical power, attributable to their quantitative properties.

Datasets and quality control (QC)

UK biobank (UKBB)

The details of assigning ancestry for each individual in the UKBB are described in the Pan-UK Biobank Project (Pan UKBB: https://pan.ukbb.broadinstitute.org/). Briefly, a random forest classifier trained on reference data from 1KG and Human Genome Diversity Project (HGDP)[48] was used to classify cohort individuals under continental population labels based on the top 6 principal components (PCs). In this study, we used a total of 361,144 and 2,684 unrelated EUR and EAS participants, respectively. We obtained unrelated individuals through running hl.maximal_independent_set using Hail (https://hail.is/). Specifically, within each population, we ran PC-Relate[49] with k = 10 and min_individual_maf = 0.05. We used the individuals assigned EAS ancestry as the target dataset. For EUR samples, we first randomly retained 5,000 individuals with complete phenotype information for all 17 studied phenotypes as the target population. Subsequently, we split the remaining individuals into evenly distributed bins, each containing 5,000 individuals, for each phenotype. The number of total bins for each studied phenotype ranged from 68 to 71, depending on phenotype missingness (Table S3). The bins were labeled sequentially from 1 to the total number of bins, following the same procedure as described in our simulations.

BioBank Japan (BBJ)

BBJ is a multi-institutional hospital-based biobank which has recruited approximately 200,000 participants from 12 medical institutions in Japan between fiscal years 2003 and 2007.[26] Written informed consents were obtained from all the participants, as approved by the ethics committees of the RIKEN Center for Integrative Medical Sciences, and the Institute of Medical Sciences, the University of Tokyo. The participants were genotyped using either (i) the Illumina HumanOmniExpressExome BeadChip or (ii) a combination of the Illumina HumanOmniExpress and HumanExome BeadChips. The genotypes were then prephased using Eagle[50] and imputed using Minimac3[51] with a reference panel that consists of 1KG samples (N = 2,504) and whole-genome sequencing (WGS) data of Japanese individuals (N = 1,037).[52] Standard quality controls of participants and genotypes were applied as described elsewhere.[52] Briefly, we excluded samples with low call rates (<98%), closely related individuals (PLINK PI_HAT >0.175), or non-Japanese outliers based on the principal component analysis (PCA). We then excluded genotyped variants with call rate <98%, HWE p-value $<1.0 \times 10^{-6}$, number of heterozygotes <5, or low concordance rate (<99.5%) with WGS for a subset of individuals (N = 939). Phenotypes were retrieved from medical records and prepared as described previously.[53]

1000 genomes project phase 3 (1KG)

We used 1KG phase 3 data as LD reference panels in this study. Specifically, we kept 495 unrelated EUR, 498 unrelated EAS, and 484 unrelated AFR individuals from 1KG. The AFR individuals were solely utilized for analyses pertaining to recently admixed populations.

Quality controls

The imputation strategies for UKBB and BBJ have been described in detail elsewhere.[27,54] After imputation, we first excluded ambiguous variants (e.g., A/T and C/G) and further filtered to keep those variants with imputation INFO score >0.3, MAF >0.01, HWE p value $>10^{-6}$, and genotyping missing rates across individuals <0.05. Consequently, approximately 8.6 million and 6.6 million SNPs were retained for the UKBB and BBJ, respectively. For our analyses, we exclusively utilized SNPs that passed these quality control measures, resulting in approximately 3.6 million SNPs that were shared among both biobanks and 1KG.

PRS construction for 17 traits in empirical analysis

Discovery GWAS

All phenotypes were curated and transformed to be normally distributed as described previously.[32] Subsequently, we performed GWAS on the rank normalized phenotypes using simple linear regression implemented in PLINK v2.0. We included age, sex, age^2, age × sex, age^2 × sex, and the first 20 PCs as the covariates. In line with the GWAS strategy outlined in the simulations section, we initially performed GWAS within individual bins and then engaged in an iterative meta-analysis, employing inverse-variance weighted meta-analysis in METAL, separately for UKBB and BBJ cohorts. For the meta-analysis of GWAS results derived from single-ancestry analyses in the UKBB and BBJ (referred to as "Meta"), we incorporated a variable number of EUR bins from UKBB, ranging from 8 to 64 with an increment of 8. Subsequently, we systematically integrated additional EAS bins from BBJ.

PRS construction methods

We used different methods to construct PRS in the target populations, specifically UKBB-EAS and UKBB-EUR. In accordance with *Simulations*, we also explored the impact of LD reference panels on PRS performance by utilizing multiple panels from 1KG, while taking into account the ancestry composition of discovery GWAS for P + T. Additionally, we implemented PRS-CS,[39] a Bayesian regression framework that integrates a continuous shrinkage prior to infer the posterior mean effects of SNPs. To alleviate computational burdens, we initially ran PRS-CS using GWAS summary statistics from UKBB with varying numbers of bins (ranging from 8 to 64, with an increment of 8) for 17 traits. We systematically explored the influence of the hyper-parameter (*phi*), representing the proportion of SNPs with non-zero effects, on PRS performance, considering diverse GWAS sample sizes and trait genetic architectures. Specifically, we performed both the grid model with various *phi* parameters (1×10^{-6}, 1×10^{-4}, 0.01 and 1) and the auto model, which automatically estimates the *phi* parameter based on the input GWAS. We used default settings for all other parameters. Our findings indicated that PRS-CS-auto exhibited comparable predictive accuracy across all traits in the UK Biobank dataset when compared to using the optimal phi parameter in the grid model (Figure S15). To ensure computational efficiency, we employed the auto model in the PRS-CS framework based on the input GWAS. For both UKBB and Meta, we used 1KG-EUR as the LD reference panel, while for BBJ, we utilized 1KG-EAS reference panel.

To further explore the performance of PRS incorporating GWAS from multiple ancestries, we constructed a weighted PRS by linearly combining PRS derived from single-ancestry GWAS.[34] Specifically, the weighted PRS was calculated as $\mathbf{PRS_{weighted}} = w_1{}^* \ \mathrm{PRS_{EUR\_GWAS}} + w_2 \ {}^* \ \mathrm{PRS_{Minor\_GWAS}}$, where w_1 and w_2 were weights attached to individual PRS. Furthermore, we used a more sophisticated method, PRS-CSx,[8] to generate ancestry-specific posterior SNP effects using multiple GWAS summary statistics. PRS-CSx, an extension of PRS-CS, can model ancestry-specific allele frequencies and LD patterns. Similar to PRS-CS, we used the ancestry-matched LD reference panel from 1KG and performed the auto model implemented in PRS-CSx. We also incorporated the –*meta* flag, which enables inverse-variance weighted meta-analysis in the Gibbs sampler. Consequently, we developed two types of PRS from PRS-CSx, one was based on the meta-analyzed effects (referred to as $\mathrm{PRS_{multi}}$) and the other, $\mathrm{PRS_{weighted}}$, was dependent on the ancestry-specific posterior SNP effects.

PRS performance evaluation

We assessed the predictive accuracy of PRS by measuring the incremental R^2 using linear regression, where we accounted for the influence of covariates. Two models were compared: 1) $H_0 : Phenotype \sim covariates$, representing the baseline model, and 2) $H_1 : Phenotype \sim PRS + covariates$, incorporating PRS as the full model. The incremental R^2 was utilized to quantify the improvement in model accuracy resulting from the inclusion of PRS, thus providing a measure of the specific contribution made by PRS to the predictive power of the model. We computed the corresponding 95% confidence intervals (CIs) through bootstrap. To maximize the predictive accuracy of P + T and $\mathrm{PRS_{weighted}}$, we employed an optimization strategy to identify the optimal p value thresholds for P + T and the weights (w_1 and w_2) assigned to various PRS components for $\mathrm{PRS_{weighted}}$. This optimization process entailed a random partitioning of the target population into two equally sized subsets, namely the validation dataset and the test dataset. The hyperparameter was identified in the validation dataset, and subsequently, the accuracy of the model was assessed using the test dataset. We replicated the process 100 times and calculated the standard error of predictive accuracy across 100 replicates. This approach allowed us to maximize the performance of P + T and $\mathrm{PRS_{weighted}}$ by iteratively refining the p value thresholds and weight parameters, thereby enhancing their predictive capabilities.

The expected accuracy of PRS in the UKBB-EAS derived from BBJ is based on the theoretical equation: $R^2 \approx \frac{h_d^2}{h_d^2 + \frac{M_d}{N_d}}$ (1),[25] where h_d^2 denotes the SNP-based heritability in the discovery population, N_d is the discovery GWAS sample size and M_d is the number of independent chromosome segments in the discovery population, which we assume to be 50,000.[55] The results are shown in Figure S14. When there is imperfect cross-ancestry genetic correlation (r_g), we used a generalization of this formula: $R^2 \approx \frac{r_g^2 h_d^2 h_t^2}{h_d^2 + \frac{M_d}{N_d}}$ (2),[36] where h_t^2 denotes SNP-based heritability in the target populations. It is important to note that this formula provides an approximation and does not explicitly account for differences in LD structure between ancestries, except for the influence of LD disparities on genetic correlation. Note that the reliability of parameter estimates such as r_g and M_d poses significant challenges, particularly in the context of multi-ancestry GWAS with highly imbalanced sample sizes.

Measures of genetic architecture using summary-data-based BayesS (SBayesS)[29]

To better understand the impact of trait genetic architecture on PRS predictive performance, we evaluated three parameters including the polygenicity (proportion of SNPs with nonzero effects), SNP-based heritability and *S* (the relationship between MAF and effect sizes) for 17 studied phenotypes (Table S3). These parameters were estimated using SBayesS implemented in the GCTB software (https://cnsgenomics.com/software/gctb/). For the analysis, we employed meta-analyzed GWAS data obtained from the comprehensive UKBB and BBJ datasets. Specifically, the number of bins included in the GWAS was equal to the total number of bins associated with the respective phenotype (Table S3). We used the LD reference panel provided by GCTB for UKBB GWAS. We constructed a shrunk LD matrix using 50,000 unrelated individuals from BBJ as the LD reference panel for BBJ GWAS. We used 4 chains for the Markov Chain Monte Carlo process, which calculated the Gelman-Rubin convergence diagnostic (also known as potential scale reduction factor) for these three parameters. We performed the analyses using other default settings for SBayesS. Given the potential convergence issues associated with Bayesian models, we deemed a threshold value of less than 1.2 for the Gelman-Rubin convergence diagnostic as indicative of good convergence for the estimated parameters.

UK biobank recent admixture ancestry analysis

To investigate one explanation for poor transferability of PRS across populations – genetic divergence between the discovery and target cohorts – we further explored whether PRS constructed from ancestry-specific summary statistics generated with local ancestry-informed GWAS in admixed populations improves predictive performance in underrepresented populations. Specifically, we used the Tractor method,[19] accounting for both local ancestry and risk allele information, to run GWAS in two-way admixed AFR-EUR individuals from the UKBB (N = 4,576). The average AFR proportion was 62.9%. We used 4,022 unrelated relatively homogeneous AFR individuals, which are independent from the admixed individuals, as the target cohort.

We followed the same criteria for QC and individual selection as described in Atkinson et al.[19] For sample QC, we excluded individuals that had <95% call rate, withdrew from the study, had closer than 2nd degree relatives present in the sample, or that had sex chromosome aneuploidies. For variant QC we restricted to biallelic SNPs with >90% call rate, HWE p value $>10^{-6}$, and MAF of at least 0.5%. We selected two-way admixed AFR-EUR individuals from the UKBB by first using the PC loadings from the reference dataset described previously for ancestry inference (1KG + HGDP) to project UKBB individuals into the same PC space. We applied the same random forest ancestry classifier described previously to the projected UK Biobank PCA data and assigned AFR ancestry if the probability was >50%. We restricted to only two-way admixed AFR-EUR ancestry individuals by selecting those individuals assigned the 'AFR' population label, then filtering to those with at least 12.5% European ancestry, at least 10% African ancestry, and who did not deviate more than 1 standard deviation from the AFR-EUR cline based on their PC loadings. This process resulted in 4,576 individuals.

We ran local ancestry deconvolution on this set of admixed individuals using RFmix v2[18] with 1 EM iteration and a window size of 0.2 cM with the HapMap combined recombination map[56] to inform switch locations. The -n 5 flag (terminal node size for random forest trees) was included to account for an unequal number of reference individuals per reference population. We used the –reanalyze-reference flag, which recalculates admixture in the reference samples for improved ability to distinguish ancestries. As a reference panel, we used continental AFR and EUR individuals from the 1KG.

Subsequently, we performed GWAS for the 17 quantitative traits utilizing the Tractor method on the 4,576 individuals with mixed AFR-EUR ancestry from the UKBB. This analysis yielded the generation of ancestry-specific summary statistics for the AFR ($\mathrm{AFR}_{\mathrm{Tractor}}$) and EUR ($\mathrm{EUR}_{\mathrm{Tractor}}$) ancestry components. To evaluate the performance of PRS in the UKBB-AFR, we developed PRS using Tractor GWAS. Furthermore, we compared these local-ancestry informed PRS with those derived from GWAS conducted using standard methodologies. Specifically, we constructed PRS using GWAS performed on the same set of admixed individuals utilizing the simple linear regression model ($\mathrm{ADM}_{\mathrm{Standard}}$). Additionally, GWAS summary statistics obtained from UKBB ($\mathrm{EUR}_{\mathrm{standard}}$, N = 320,000) from the previous section were utilized, and a meta-analysis was conducted to combine the $\mathrm{AFR}_{\mathrm{Tractor}}$ with $\mathrm{EUR}_{\mathrm{standard}}$ ($\mathrm{Meta}_{\mathrm{standard}}$, N = 324,576). We constructed PRS based on HapMap3 SNPs, as previous studies have shown comparable performance between using reliable HapMap3 SNPs exclusively and the use of genome-wide SNPs.[7,57] Additionally, we constructed weighted PRS by incorporating GWAS of $\mathrm{AFR}_{\mathrm{Tractor}}$ and $\mathrm{EUR}_{\mathrm{Standard}}$, for P + T, PRS-CS and PRS-CSx, respectively. Considering the ancestry composition of the discovery GWAS, we used different sets of reference panels for each respective GWAS. Specifically, we used 1KG-EUR as the LD reference panel for $\mathrm{EUR}_{\mathrm{Tractor,}}$ $\mathrm{EUR}_{\mathrm{standard}}$ and $\mathrm{Meta}_{\mathrm{standard}}$, while using 1KG-AFR for $\mathrm{AFR}_{\mathrm{Tractor}}$. We used an in-sample LD panel for $\mathrm{ADM}_{\mathrm{Standard}}$. We calculated the predictive accuracy in the UKBB-AFR using incremental R^2 as described above. We repeated the process 100 times and reported the standard error of predictive accuracy across 100 estimates.

Given that heritability bounds predictive accuracy, which can vary among populations and contexts, we also compared SNP-based heritability estimates between the AFR and EUR populations in the Pan-UK Biobank Project (https://pan.ukbb.broadinstitute.org/docs/heritability/index.html).